PONTIFICIA UNIVERSIDAD CATOLICA DE CHILE

ESCUELA DE INGENIERIA

MEASUREMENT OF THE EQUILIBRIUM PARTITION OF TOMATO OLEORESIN BETWEEN SUPERCRITICAL CO_2 AND SELECTED ADSORBENTS USING DYNAMIC METHODS

SOFÍA P. ANDRIGHETTI FERRADA

Thesis submitted to the Office of Research and Graduate Studies in partial fulfillment of the requirements for the Degree of Master of Science in Engineering

Advisor:
JOSÉ M. DEL VALLE

Santiago de Chile, (December, 2014)

PONTIFICIA UNIVERSIDAD CATOLICA DE CHILE
ESCUELA DE INGENIERIA

MEASUREMENT OF THE EQUILIBRIUM PARTITION OF TOMATO OLEORESIN BETWEEN SUPERCRITICAL CO_2 AND SELECTED ADSORBENTS USING DYNAMIC METHODS

SOFÍA P. ANDRIGHETTI FERRADA

Members of the Committee:

JOSÉ MANUEL DEL VALLE LLADSER

LORETO VALENZUELA ROEDIGER

GONZALO NÚÑEZ MONTOYA

CRISTIÁN ESCAURIAZA MESA

Thesis submitted to the Office of Research and Graduate Studies in partial fulfillment of the requirements for the Degree of Master of Science in Engineering

Santiago de Chile, (December, 2014)

To my parents and my boyfriend, for their support and patience. We did it!!

ACKNOWLEDGEMENTS

I would like to thank to FONDECYT project Nº 1111008 for providing the economic resources needed for this thesis development.

I also want to thank Professor José Manuel del Valle for trusting me, guiding me, and helping me in the development of this thesis. Thanks to the committee members Loreto Valenzuela for introducing me to researching, Gonzalo Núñez for supporting and teaching me, and Cristián Escauriaza for his great disposition.

I am very grateful of members of Laboratorio de Extracción de Materiales Biológicos: Gonzalo Nuñez, Fabián Reyes, Arturo Bejarano, Caroline Sielfeld, Soledad Murias, Julia Arango, Natalia Carathanassis and Christopher Lorca, for accompanying me and helping me answering my questions. I am especially thankful of Eduardo Richter for his willingness and patience in helping me. Last but not least I am very thankful of Freddy Urrego for teaching me, guiding me in the use of the equipment, and his excellent willingness in answering all my questions. Thanks them all for the great patience they had: this thesis is definitely yours too.

I am very thankful of the people that work in the Departamento de Ingeniería Química y Bioprocesos. Thank you for making of the Department, a friendly place.

Last but not least, to my parents, sisters and boyfriend. Thank you for your endless patience and support during this trip.

For all the previously mentioned people, remember that:

If I have seen further it is only by standing on the shoulders of giants

– Isaac Newton

GENERAL INDEX

Pag.

DEDICATORY ii

Acknowledgements iii

List of tables vi

List of figures vii

ABSTRACT ix

RESUMEN x

1. Introduction 1
   1.1 Objective 3

2. Literature survey 4
   2.1 Adsorption concept applications: a review 5
      2.1.1 Gas storage and sequestration 5
      2.1.2 Textile dyeing 8
      2.1.3 Soil remediation 11
      2.1.4 Adsorbent regeneration 13
      2.1.5 Cleaning or reconditioning of supercritical fluids 14
      2.1.6 Preparative chromatography 16
   2.2 Sorption isotherms 18

3. Materials and methods 21
   3.1 Tomato oleoresin samples 21
   3.2 Adsorbent selection 22
   3.3 Adsorbent assessment 24
   3.4 Statistical analysis 28

4. Results and discussion 29
   4.1 Adsorbent selection 29
   4.2 Sorption isotherm 33

5. Conclusions 47

REFERENCES 49

NOMENCLATURE 62

APPENDIXES 63

Appendix A: Frontal analysis in steps 64

Appendix B: Porosity estimation 65

LIST OF TABLES

Pag.

Table 3.1: Characterization of the adsorbents considered in this work..... 23

Table 4.1: Isotherm coefficients..... 45

LIST OF FIGURES

Pag.

Figure 1.1: Molecular structure of lycopene 2

Figure 3.1: Isotherm measurement equipment 26

Figure 4.1: Spectrophotometer response for samples at different tomato oleoresin concentrations in hexane 29

Figure 4.2: Spectrophotometer response for samples with different adsorbents 31

Figure 4.3: Visual comparison of adsorbents 32

Figure 4.4: Tomato oleoresin concentration in chitosan in microspheres and silica gel 33

Figure 4.5: UV-Vis response to different oleoresin concentrations in SC CO_2, with column filled with glass beads 34

Figure 4.6: Relation between oleoresin concentration in the SC phase, and UV-Vis response 35

Figure 4.7: Reproducibility of calibration curve assessing by running the experiment using 13% of saturation concentration in triplicate 36

Figure 4.8: Standard calibration curve 37

Figure 4.9: UV-Vis response to tomato oleoresin 28% saturation concentration in SC CO_2, with a column filled with 1 mm of silica gel 38

Figure 4.10: Reproducibility of adsorbent experiments 39

Figure 4.11: Chitosan packed bed before and after the breakthrough curves experiments 40

Figure 4.12: UV-Vis response with chitosan in microspheres together with their standard calibration curve 41

Figure 4.13: Oleoresin concentration in solid and fluid phases 43

Figure 4.14: Best and worst fitted isotherm 44

Figure 4.15: Prolongation of the four isotherm models 46

Figure A.1: Frontal analysis in steps 64

ABSTRACT

Supercritical (SC) carbon dioxide (CO_2) has been studied as an alternative for solvent extraction due to their beneficial properties. The solubility of natural compounds in SC CO_2 varies depending on working conditions, making it a selective solvent. Because traditional separation in SC extraction by decreasing pressure or modifying temperature is an intensively energy-demanding process, adsorbents have been proposed as an alternative for solvent recycling. Adsorption and desorption using SC CO_2 has been studied for gas adsorption, fibre dyeing, adsorbent regeneration, and compound separation and concentration, applications that are reviewed in this thesis.

The interaction between adsorbent and solute is a key factor in oleoresin recovery maximization. The hypothesis of this work is that only selected adsorbents are appropriate for oleoresin recovery, thus the objective was to identify an appropriate adsorbent for the separation of tomato oleoresin and to measure oleoresin partition between selected adsorbents, and SC CO_2. To select the best adsorbent this work compared activated carbon, silica gel, chitosan in microspheres, celite, and microcrystalline cellulose by dissolving tomato oleoresin in hexane and measuring their adsorption at 40 ºC as a function of oleoresin concentration. Selected adsorbents were chitosan in microspheres and silica gel with intermediate affinity to oleoresin.

To measure equilibrium partition of oleoresin between selected adsorbents and SC CO_2 at 40 ºC and 28 MPa in a packed bed this work used a dynamic method. Equipment restrictions made it impossible to measure silica gel equilibrium partition. In the case of chitosan, an irreversible adsorption and low interaction were observed. Isotherms were measured using methods based on mass balances and breakthrough curves. Differences between methods may be due to imprecisions in breakthrough curves due to oleoresin fractionation. Differences in solute content in the solid between adsorption and desorption may be due to difficulties in keeping the equilibration subsystem saturated. The method based on mass balances worked best because it considered fractionation.

Keywords: Supercritical fluids, Carbon dioxide, Adsorption, Equilibrium partition.

RESUMEN

El dióxido de carbono (CO_2) supercrítico (SC) ha sido estudiado como alternativa a la extracción con solventes por sus propiedades beneficiosas. La solubilidad de compuestos naturales en CO_2 SC varía con las condiciones de trabajo, siendo un solvente selectivo. Como el proceso de separación tradicional en extracción SC por descompresión o cambio de temperatura es demandante de energía, se propone la adsorción como alternativa para separar y reciclar el solvente. La adsorción y desorción en adsorbentes y compuestos relacionados usando CO_2 SC se aplica en adsorción de gases, teñido de fibras, remediación de suelos, regeneración de adsorbentes, y separación/concentración de compuestos, aplicaciones que son revisadas en esta tesis.

La interacción con el adsorbente es clave para maximizar la recuperación del extracto. La hipótesis del trabajo es que algunos adsorbentes son apropiados para la recuperación del extracto, así el objetivo fue identificar un adsorbente adecuado y medir la partición de oleorresina de tomate entre el adsorbente escogido y CO_2 SC. Para seleccionar el adsorbente se comparó carbón activado, silica gel, quitosano en microesferas, celita, y celulosa microcristalina disolviendo la oleorresina en hexano y midiendo la adsorción a 40 ºC, en función de su concentración. Los adsorbentes escogidos fueron quitosano y silica gel con afinidad intermedia a la oleorresina.

Se usó un método dinámico para medir el equilibrio de partición de la oleorresina entre el adsorbente empacado y CO_2 SC a 28 MPa y 40 ºC. Limitaciones en el equipo impidieron la medición de la partición de silica gel. Con quitosano se observó una adsorción irreversible y baja interacción. Las isotermas se midieron con métodos basados en balances de masa y curvas de ruptura. Sus diferencias se explican con imprecisiones en curvas de ruptura por el fraccionamiento de la oleorresina. Diferencias de concentraciones en el sólido entre adsorción y desorción se explican por dificultades en mantener saturado el subsistema de equilibrio. El método de balances de masa funcionó mejor ya que considera el fraccionamiento.

Palabras Claves: Fluídos supercríticos, Dióxido de carbon, Adsorción, Equilibrio de partición.

1. INTRODUCTION

Components of a solid matrix have been separated using solvents (solid-liquid extraction or lixiviation) since immemorial times. In this process the solvent dissolves one or more soluble components in the solid matrix (insoluble) (McCabe & Smith, 1969). Traditional extraction processes for food, pharmaceutical, and other industries use organic solvents such as ethanol, acetone, or petroleum ether among others (Periago et al., 2004). Some of these solvents could be toxic and moreover heat might be required for the separation of the solvent and compound of interest by, *e.g.*, distillation. In this context supercritical (SC) fluids (SCFs) and especially SC carbon dioxide (CO_2) is being increasingly used for extraction processes due to their desirable properties: solvent properties comparable to those of liquids, and transport properties comparable to those of gases. Because solubility in SC CO_2 is highly dependant on extraction conditions, SC CO_2 can be very selective (del Valle & Aguilera, 1999). Moreover, because CO_2 is inert, non-toxic, and has a near-ambient critical temperature (31 ºC) (NIST, 2011), it is suitable for extracting thermolabil compounds (Saldaña et al., 2010).

In SC CO_2 extractions, steep changes in system pressure (preferably) and/or temperature can be applied to precipitate out dissolved natural compounds in a separator prior to recycling the SC CO_2 to the extractor. This type of separation consumes a lot of energy and constitutes a process limitation at the industrial level. This can be avoided using an adsorbent where the dissolved natural compounds can be selectively removed from the SC CO_2 stream at constant temperature and pressure (Jüntgen, 1977). It is possible to take advantage of this selective adsorption for sample analysis purposes in SC CO_2 chromatography. Relative affinity of the components of the sample between the adsorbent (stationary phase) and SC CO_2 (mobile phase) determines their migration velocity in a packed column (they come out of the column separately) (Brunner & Johannsen, 2006).

To fully take advantage of an adsorbent using SC CO_2 it is necessary knowing the equilibrium partition of a solute (or solute mixture) between the two phases as a

function of the systems conditions (temperature and pressure). The equilibrium partition may be relevant in the selection of adsorbents for H_2 storage in fuel cells (Chambers et al., 1998; Dillon et al., 1997; Ströbel et al., 2006), sequestration of CO_2 in geological formations (de Silva et al., 2012; IPCC, 2005; Perera et al., 2010; White et al., 2005), textile dyeing (Banchero, 2012), soil remediation (Sunarso & Ismadji, 2009), adsorbent regeneration (Tan & Liou, 1989a, b; Zhu et al., 2009), cleaning or reconditioning of SCFs (Brunner & Johannsen, 2006; Madras et al., 1994), and analytical and preparative chromatography (Guiochon & Tarafder, 2011; Miller, 2012). The equilibrium partition can be measured using a static method in which SC CO_2 is recirculated through the packed bed with the adsorbent, up to reaching equilibrium (Urrego et al., 2011, 2012), and using a dynamic method such as frontal analysis (Brunner & Johannsen, 2006). The first one tends to be more time consuming; thus this thesis uses a dynamic method.

In this work, tomato oleoresin is used as a model natural mixture, because of its high-content of value-added bioactive carotenoids such as lycopene (Fig. 1.1). Lycopene content in tomato ranges 8.8 - 42.0 μg/g (wet basis) (Rao & Rao 2007). It confers red colour to tomato oleoresin, being easily quantifiable by measuring its UV-Vis absorbance. Lycopene is an acyclic tetraterpene formed by four isoprene units, having eleven conjugated double bonds arranged in an all-trans configuration in nature (Bramley, 2000). Because lycopene can neutralize singlet oxygen and peroxyl radicals (Gómez-Prieto et al., 2003; Ollanketo et al., 2001; Saldaña et al., 2010; Shi et al., 2009), it has been recommended as a nutraceutical to prevent certain illnesses such as coronary diseases and different types of cancer (Bramley, 2000).

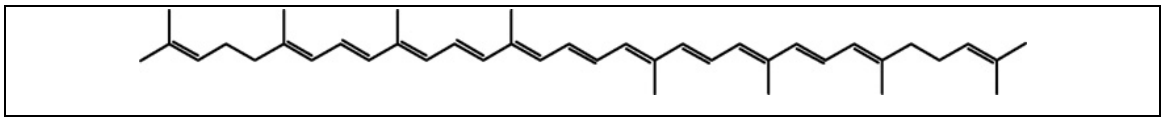

Figure 1.1: Molecular structure of lycopene (Shi et al., 2009)

The nonpolar nature of lycopene hinders its extraction using polar solvents such as water. On the other hand, there have been recommendations to substitute conventional organic solvents by SC CO_2 for the extraction of tomato oleoresin (Zuknik et al., 2012), because it is very heat-labile and tends to oxidize with oxygen (Henry et al., 1998).

There have been studies on equilibrium partition of pure substances, but there are only a few on the use of adsorption for the selective recovery of plant carotenoids in SC CO_2 extraction processes (Ambrogi et al., 2002, 2003). Ambrogi et al. (2003) compared two adsorbents (bleaching earth and silica gel) to recover carotenoids (natural colorants) for from paprika oleoresin using an extraction-adsorption process. They concluded that solute interaction with the adsorbent should be lower in order to have an efficient recovery process. Thus, they recommended carrying out additional experiments with organic adsorbents such as cellulose.

1.1 Objective

The general objective of this work was to identify an adsorbent with adequate affinity for carotenoids in tomato oleoresin, and to study their partition with SC CO_2. The specific objectives were:

a) To compare different adsorbents (activated carbon, microcrystalline cellulose, chitosan in microspheres, celite, and silica gel), using hexane as solvent, and selecting the most adequate ones.

b) To measure the equilibrium partition of tomato oleoresin between SC CO_2 and selected adsorbents, at 40 ºC and 28 MPa.

The following chapter of this thesis reviews applications of adsorption in SCF and overviews frontal analysis as a method to obtain sorption isotherms. The rest of the thesis has the conventional organization of a research article including experimental methods, results, and discussion.

2. LITERATURE SURVEY

Adsorption is the process in which molecules from a fluid phase adhere to the surface of a solid phase due to the interaction between atoms or functional groups (Brunner & Johannsen, 2006). Molecules from the fluid phase attach the adsorbent's so-called active sites due to physical forces generated by their electronic structure (Jüntgen, 1977). Desorption is the inverse process in which adsorbed molecules are removed from the solid phase, by a fluid.

Adsorption may be understood both as an on-off process, in which the solute is divided in two fractions: one retained by the adsorbent and the other non-retained, and as a chromatographic process: multiple adsorption-desorption steps (Brunner & Johannsen, 2006) where different components of a mixture are carried by a mobile phase (fluid phase) at different speeds. There are mass transfer processes between the solid phase and the fluid phase, in which different components of the mixture have different affinities with the adsorbent. Both the solvent power of the fluid phase and the relative affinity of each component with the solid phase determine how the mixture interacts with the adsorbent, and their concentration in each phase, particularly in the fluid leaving the system as the outlet stream.

The total amount of molecules adsorbed depends on their initial concentration in the fluid phase (Jüntgen, 1977), and there is an interaction between the fluid phase and the adsorbent (del Valle & Urrego, 2012). This implies that there exists equilibrium partition of solutes between the phases. The equilibrium is reached when at constant temperature, pressure, and concentration of the solute in the fluid, a specific fraction of active zones is occupied by adsorbed molecules (Jüntgen, 1977). This interaction is described using sorption (adsorption/desorption) isotherms, which are functions that describe solute concentration in both adsorbent and fluid phase.

Adsorption is not always a totally reversible process, in that there may be a residual fraction of molecules adsorbed in systems with high adsorption energy (Jüntgen, 1977). To revert the adsorption process, it might be necessary to change the operational conditions of SC CO_2 (pressure, temperature, and/or mass flow).

2.1 Adsorption concept applications: a review

Previous reviews have shown many applications of the adsorption concept with SCFs. Lee & Cochran (1992) and Aranovich & Donohue (1996) mentioned that SCFs are used in adsorption science for different purposes such as textile dyeing, adsorbent regeneration, soil remediation, and separation of components with the aim of eliminate or concentrate compounds. This chapter briefly describes some of them.

There is a large variety of adsorbents that can be used for different applications according to the specific needs of the process. Some adsorbents are mostly used with polar compounds, and others with non-polar compounds. There is no review or summary of adsorbents commonly used with SC CO_2, but Dettmer & Engewald (2002) reviewed adsorbent materials used for adsorption of volatile organic compounds (VOCs). They identified three types of adsorbents: inorganic adsorbents such as silica gel, zeolites, and alumina that are used mainly for polar compounds; and carbonaceous adsorbents such as activated carbon; and organic polymers adsorbents such as chromosorb, that are both suitable for organic compounds.

2.1.1 Gas storage and sequestration

Gas adsorption has been studied both with the aim of using the gas, and to keep it out of the atmosphere. Hydrogen (H_2) has been studied as a cleaner alternative for fossil fuels. Benefits include its regenerability using electrolysis, where the only residue is water, and its high heating value (Vasanth Kumar et al., 2010).

In H_2-based fuel-cell vehicles, storing H_2 is an important issue because of its complexity (Wu et al., 2009). H_2 storage has been studied into different types of carbon (Ströbel et al., 2006) such as activated carbon (Monteiro de Castro et al., 2010), carbon nanotubes (Chen et al., 1999; Dillon et al., 1997), graphite fibres (Chambers et al.,1998), and other adsorbents.

Zhou & Zhou (1996) studied H_2 adsorption into activated carbon. They observed that the adsorption capacity of carbon for H_2 was not affected by multi-repetition of

adsorption-desorption cycles; this is also claimed by Ströbel et al. (2006). According to Zheng et al. (2005) lower temperatures increased the capacity of multi-walled carbon nanotubes to adsorb H_2. Although they observed that adsorption temperature was related to H_2-H_2 interaction energy, they concluded that it does not give information about optimal temperature for H_2 storage in multi-walled carbon nanotubes. Zhou & Zhou (1996), observed that H_2 was less adsorbed at higher temperatures, whereas Zubizarreta et al. (2008) observed that temperature influenced more than pressure carbon adsorption capacity.

Murata et al. (2002) studied SC H_2 (T_c = -239 ºC and P_c = 1.3 MPa) adsorption into internal and interstitial nanospaces of a single-wall carbon nanohorn assembly. They concluded that the density of adsorbed H_2 in interstitial spaces between particles is lower than in internal spaces within particles due to the self-stabilization effect related to cluster formation of H_2 and strongly adsorbed molecules. Zubizarreta et al. (2008) concluded that physisorption (adsorption due to intermolecular forces) is the main process involved in H_2 storage, and that gravimetric storage capacity depend on textural properties rather than on morphology of the adsorbent.

Sudibandriyo (2011) studied high-pressure adsorption of methane (CH_4) and H_2 on activated carbon. He observed that CH_4 was more adsorbed than H_2. He attributed low H_2 adsorption to activated carbons pore size, and suggested that reducing it may improve H_2 adsorption.

The increasing concentration of greenhouse gases in the atmosphere has driven efforts to explore mechanisms to diminish them. CO_2 sequestration into geological adsorbents is proposed for long-term storage (de Silva et al., 2012; IPCC, 2005; Perera et al., 2010; White et al., 2003, 2005). Some sequestration methods are underground unminable coal seam, active or depleted oil and gas fields exploited using enhanced oil recovery (EOR) or enhanced gas recovery (EGR) methods, and deep saline aquifers, among others (de Silva et al., 2012; IPCC, 2005). In most cases, physical and geochemical mechanisms inhibit the migration of CO_2 back to the surface, however CO_2

storage in coal beds may occur due to physical adsorption within pores and molecular structures (White et al., 2005). This section only covers underground coal seams.

CO_2 can be used for EGR in coal beds, because they tend to have CH_4 adsorbed. The coal matrix adsorbs CO_2 making the matrix releases CH_4 (Bachu, 2000). This process not only permits the sequestration of large amounts of CO_2 but also improves CH_4 extraction and profitability of natural gas operations (Reichle et al., 1999). There are some properties of coal that affect the sequestration process including carbon content, moisture, substrate chemistry, and surface area-to-volume ratio (Perera et al., 2010; Viete & Ranjith, 2006).

Carbon content increases the rank of the coal (Perera et al., 2010). According to Puri & Yee (1990), for every mole of CH_4 desorbed in a medium-to-high rank coal, two moles of CO_2 can be adsorbed, and according to Stanton et al. (2001), low rank coal could adsorb ten moles of CO_2 for every mole of CH_4 desorbed (White et al., 2005), although this ratio could increase with higher pressures because CO_2 may turn into SC state (White et al., 2005).

Moisture affects the capacity of coals to sequester CO_2, because it could affect its strength and capacity to avoid migration of CO_2 back to the atmosphere. Krooss et al. (2002) studied CH_4 and CO_2 adsorption on dry and moisture-equilibrated Pennsylvanian coals. They observed that for dry coal in most cases CO_2 was better adsorbed at 40 ºC than at higher temperatures. In moisture-equilibrated coals they observed a great difference in behaviour at different pressures. They also observed that, above 100 bar, the adsorption capacity of coals for CO_2 increased with pressure. Clarkson and Bustin (2000) suggested that selectivity towards CO_2 is greater for dry coals.

Adsorption not only depends on adsorbents characteristics but also on temperature and pressure. Hall et al. (1994) studied adsorption of CH_4, N_2, CO_2, and their mixtures into wet fruitland coal. They concluded that above 96.5 bars, CO_2 adsorption into coal increase. Pashin & McIntyre (2003) studied the effect of temperature and pressure conditions in coal bed CH_4 reservoirs of the Black Warrior

basin, and concluded that if SC conditions developed, increasing pressure would stimulate undersaturation of coal, because coal can hold large quantities of SC CO_2.

Coals have a polymer-like matrix structure, consequently their characteristics such as permeability, could vary if contacted with gases or solvents (White et al., 2005). Viete & Ranjith (2006) studied the effects of CO_2 sequestration on permeability and geochemical behaviour of brown coal. They concluded that adsorption causes a decrease in coal strength. Their results suggest an association between CO_2 adsorption and coal's strength. They also concluded that the introduction of CO_2 in the coal seam may weaken it inducing fractures that may disable the coal to sequester CO_2 (Viete & Ranjith, 2006). Upon CO_2 desorption, coal shrinks and conversely CO_2 adsorption swells it (Siriwardane et al., 2009). Coal fractures might increase or decrease due to shrinkage or swelling, thus its permeability changes (Siriwardane et al., 2009).

Coal beds are at lower depths than other storage sites, and storage of CO_2 in deep geological formations uses technologies already developed for the oil and gas industry, however technical feasibility largely depends on the permeability of the coal bed (IPCC, 2005). According to Stevens et al. (2001) the applicability of enhanced coal bed CH_4 recovery has not been demonstrated at pilot scale yet. Zhou et al. (2013) studied the feasibility of enhanced recovery of CH_4 in a coal bed, and CO_2 storage in Southeast Qinshui Basin in China. They concluded that gas injection yields increases CH_4 recovery independent on the composition of injected gas. Liu et al. (2013) developed a model to assess feasibility of storing CO_2 in New Albany Shale with EGR. They suggested that CO_2 injection could be technically feasible and it could sequester CO_2 effectively by adsorption. Gas adsorption was found to be the dominant sequestration mechanism (Liu et al., 2013).

2.1.2 Textile dyeing

Traditional dyeing processes use large amounts of water. Furthermore they require dispersing and surfactant agents to improve dye uptake; therefore the entire process (including washing procedures) discharges large amounts of wastewater. SC CO_2 has been proposed as an alternative to decrease the environmental impact of the

process by dissolving the dye into SC CO_2 prior to transferring it to the fibre. However the non-polar nature of CO_2 represents a challenge on dyeing hydrophilic fibres (Banchero, 2012).

Nowadays many fibres used commercially are made from synthetic polymers. Different polymers have different sorption behaviour in presence of CO_2, depending on the molecular composition and structure of the polymer, and the conditions of the CO_2 (Shieh & Liu, 2003). Sorption of gases into polymers has an associated effect of polymer swelling, which is studied for different processes (Pantoula et al., 2007).

CO_2 sorption behaves different on polymers depending on their glass transition temperature (T_g) (Tomasko et al., 2003) The T_g is the temperature at which a second order phase change (from liquid-like rubbery to solid-like vitreous) occurs to an amorphous solid: when heated, the vitreous solid becomes rubbery and soft, and when cooled, the rubbery liquid becomes glassy and brittle. When polymeric fibres are in contact with the dyeing bath, CO_2 molecules can penetrate into the free volume of the amorphous parts of the polymer having a plasticization effect, which results on a reduction of T_g (von Schnitzler & Eggers, 1999). This was also observed by Hou et al. (2010) while dyeing polyethylene terephthalate (PET) fabric using SC CO_2. After reaching equilibrium (when the dyeing process was over), CO_2 removed excess dye by decreasing the temperature below T_g to avoid extracting fixed dye from the fibre. They observed that below T_g, colour yield (relation between absorbance and scattering coefficient of the substrate) was similar to that in a traditional dyeing process. On the other hand, colour yield was lower above T_g.

Park et al. (2010) observed that depending on the type of polymer, an increase in pressure or temperature improve dye sorption. They suggested that both the type of interaction between dye and polymer, and the amount of amorphous spaces, affect sorption. They observed that sorbed dye decrease with the crystallinity of the polymers. West et al. (1998) observed that despite the limited solubility of dyes in CO_2, they are well uptaked by the polymer. Thus, solubility is not the only governing factor in

polymer dyeing, but also the relative affinity of the dye to the polymer and the CO_2 (West et al., 1998).

Regarding working temperature, Özcan & Özcan (2005) concluded that SC dyeing could be carried out at lower temperatures than traditionally in polyester. They observed that dye uptake is best at 95 ºC while the traditional dyeing temperature is around 130 ºC. They attributed it to the improved diffusion of the dyes within the polymer when using SC CO_2.

van der Kraan et al. (2007) studied dyeing of natural and synthetic textiles (silk, wool, polyester, and nylon) with disperse reactive dyes dissolved in SC CO_2. They observed that higher moisture content on CO_2 and/or in the textile improve dye uptake depending on the type of dye and textile. This was attributed either to water ability to swell fibres or to its interaction with the dye-fibre system.

Fibres such as wool or cotton are more difficult to dye because CO_2 cannot swell them (Banchero, 2012) and because they are polar (Bach et al., 2002). As a consequence, fibres do not uptake an appropriate amount of disperse dyes, and polar dyes (used in common dyeing processes) do not solubilize well into SC CO_2 (Bach et al., 2002). To improve dye capture by natural fibres, physical and chemical pretreatments have been proposed (Bach et al., 2002; Banchero, 2012).

Physical pretreatment has been studied to improve dye uptake by natural fibres. Plasticizing agents such as ethylene glycol appear to improve dye uptake in cotton (Beltrame et al., 1997). Guzel & Akgerman (2000) created mordant wool by adsorbing/ion-exchanging a metal ion to the fibre from an aqueous solution, and used mordant dyes (dyes with chelating agent) dissolved into the SC CO_2. The dyes reacted with the surface of the modified fibre. They concluded that with moistured wool, the treatment work better. The optimal conditions and process time depended on dye solubility into SC CO_2 and the pH of the aqueous medium (Guzel & Akgerman, 2000).

Chemical pre-treatments have been studied also to improve the uptake of dyes by natural fibres. Özcan et al. (1998b) pretreated cotton by reaction with benzoyl chloride and used dispersed dyes. They observed good colour intensity. Özcan et al. (1998a)

studied cotton pre-treated with benzoyl chloride, or sodium benzoylthioglycollate. They observed that the first agent, although effective, caused an important gain of weight. Using the second agent they observed a less satisfying dyeing results, however they concluded that it is possible to dye cotton using SC CO_2. While studying SC dyeing of cotton modified with 2,4,6-trichloro-1,3,5-triazine, Schmidt et al. (2003) observed that modified cotton could be dyed using SC CO_2. They suggest that to achieve dye uptake, this has to contain a group such as hydroxyl or amino that could react with the fibre reacting group. They used water and acetone as solvents to modify cotton. They observed higher colour depths using water; nevertheless it decreases the speed of washing. Liu et al. (2006) studied ramie fibre dyeing modifying it with a two-step process using alkali and benzoyl chloride. Although pre-treatment caused some damage to the fibre, they observed good colour yields and washing speeds which increased with pressure, temperature, and time.

2.1.3 Soil remediation

There are many studies on the extraction of toxic organic compounds, herbicides, and pesticides from soil with SCFs, because traditional solvent extraction is not considered good for the environment. Contaminants in soil can be in an adsorbed and/or a deposited state. Contaminants in deposited state are not difficult to remove by dissolving them in the SC phase, whereas those in adsorbed state, could be hard to remove because removal is controlled by sorption equilibria (Erkey et al., 1993; Sunarso & Ismadji, 2009). This technology creates small waste volume and thus an organic concentrate. This improves subsequent treatment processes (Brady et al., 1987).

There are several studies on remediation of soil contaminated with petroleum hydrocarbons. Erkey et al. (1993) studied adsorption isotherms of naphthalene, phenantrene, hexachlorobenzene, and pentachlorophenol dissolved in liquid and SC CO_2 into soil. The aim of this study was to propose SC CO_2 desorption as an alternative for soil decontamination. Nagpal & Guigard (2005) studied the extraction of petroleum hydrocarbons from flare pit soils by using SCF. They concluded that extraction efficiency increase when increasing pressures and decreasing temperatures. Efficiency

was better with coarse-grained sand (Nagpal & Guigard, 2005). Hawthorne & Miller (2003) studied sequestration of benzene; toluene; ethylbenzene; o-, m-, and p-xylene; and polycyclic aromatic hydrocarbons (PAHs) from soils abandoned for several decades. They observed that the slowest compound to be removed from all samples was benzene because it was tightly sequestrated. Young & Weber (1997) studied interactions between phenanthrene and five natural materials. They concluded that differences in extraction efficiency could be related to matrix-analyte interactions. They observed that increasing temperature was more effective than increasing pressure in improving desorption.

Berglöf et al. (1998) extracted metsulfuron methyl, sulfometuron methyl, and nicosulfuron herbicides from soils. They observed that the recovery of herbicides diminished as the concentration of organic carbon and clay increased in soil. They suggested that optimized conditions cannot be applied to similar components sorbed in different matrices without further study.

Brady et al. (1987) extracted polychlorinated biphenils, toxaphene, and dichlorodiphenyltrichlorethane (DDT) extraction from both topsoils and subsoils. They concluded that process efficiency depends mostly on the content of organics and water in soil. Zhou et al. (1997) studied extractability of pesticides. They observed that the time the pesticide resided in the soil greatly influenced its extractability. They also observed that different parameters such as organic carbon and clay content affected the different types of pesticides in various ways. Modifiers and extraction time also affected extractability of "aged" pesticides. Sahle-Demessie & Richardson (2000) compared SCF extraction with solvent extraction and low temperature thermal desorption of DDT, dichlorodiphenyldichloroethane (DDD), toxaphene, hexachlorocyclohexane, and dichlorodiphenyldichloroethylene (DDE). They observed that with higher amounts of fine particles, the extraction efficiency diminishes. A decrease in extraction rate is observed as moisture increases. They also observed that SCF extraction reduced residues volume.

There have been several comparative studies on the efficiency of soil remediation methods. Wright et al. (1989) compared Soxhlet and SCF extraction of PAHs from soil

contaminated with coal tar. They observed high extraction efficiency at the first 30 minutes, but that high molecular weight PAHs were not well extracted because of their low solubility in SC CO_2. Dean et al. (1995) studied three extraction methods: Soxhlet, microwave, and SCE for sixteen PAHs from a native contaminated soil, they observed that SCE was the most effective, and showed considerations such as costs and operator skills. Dupeyron et al. (1999) compared five types of extraction: microwave assisted, SC, subcritical solvent, sonication, and Soxhlet, and concluded that sonication and Soxhlet extraction are less effective than the others and that differences among the three others are mainly practical. Bernal et al. (1996) compared SCF with solvent extraction. They observed that SCF extraction was not fully effective in aged soils, unlike solvent extraction. They observed that using a modifier, extraction could improve.

2.1.4 Adsorbent regeneration

Adsorbent regeneration is widely studied in order to recover and re-use adsorbents. Tan & Liou studied SCF regeneration of activated carbon loaded with ethyl acetate (Tan & Liou, 1988), toluene (Tan & Liou, 1989a), and a mixture of benzene and toluene (Tan & Liou, 1989b). These studies showed that regenerated adsorbents maintained their original adsorbent properties close to the original levels. Authors observed that the regeneration was better at higher pressures, and concluded that regeneration using SC CO_2 is more favourable than using water vapour.

Adsorption equilibrium might play an important role in desorption. Macnaughton & Foster (1995) studied DDT adsorption and desorption on activated carbon using SC CO_2. They observed that DDT desorption was not favourable because there was less than 60% removal. At the highest flow rate, they could not achieve the equilibrium. Madras et al. (1993) studied SCF regeneration of activated carbon loaded with heavy molecular weight organics. They used chromatographic techniques. They observed that regeneration capability depends on the solubility of the compounds in SC CO_2, however it might also depend on adsorption equilibrium. Macnaughton & Foster (1995) concluded that adsorption equilibrium might be the limiting step. Activated carbon

regeneration is made difficult by the affinity between organic compounds and activated carbon, which means a low regeneration rate (Salgın et al., 2004).

Organoclays are clay minerals whose inorganic ions are replaced under certain conditions with organic ions (Frost et al., 2008; Zhu et al., 2009). This changes clay from having affinity to hydrophilic to hydrophobic compounds, thus organoclays are useful sorbents for organic compounds disposed in water (Huang et al., 2007; Zhou et al., 2007a, b). They can be used to prevent percolation of organic pollutants into ground water (Brixie & Boyd, 1994; Lo & Yang, 2001; Zhu et al., 2009) as well as to remove organic pollutants from air (Shu & Su, 2002; Tian et al., 2004; Volzone et al., 2006). There are different methods to regenerate organoclays including biological degradation, chemical extraction/desorption, thermal desorption, and SCF extraction (Zhu et al., 2009).

There have been studies testing adsorption of organic compounds into organoclays and the capacity of SC CO_2 to regenerate them when charged with salicylic acid (Salgın et al., 2004), phenols (Park & Yeo, 1999), and ethyl acetate (Cavalcante et al., 2005; Coelho et al., 2001). Salgın et al. (2004) used ethanol as cosolvent to regenerate organoclays charged with salicylic acid. They observed that desorption effectiveness improved when increasing temperature, pressure, SC CO_2 mass flow, and cosolvent concentration. Park & Yeo (1999) showed that the regenerated organoclay apparently did not loose its adsorption power after three phenols adsorption-desorption cycles. Coelho et al. (2001) concluded that desorption of ethyl acetate decrease its efficiency as temperature increases. Cavalcante et al. (2005) observed that desorption of ethyl acetate was better using SC CO_2 than high-pressure CO_2, and proposed SC CO_2 desorption as an effective technology for organoclay regeneration.

2.1.5 Cleaning or reconditioning of supercritical fluids

One application of adsorption-desorption process is related to the cleaning or reconditioning of SCF or to recover compounds dissolved in SC CO_2 after extraction in a solid matrix: the adsorbent. According to Brunner & Johannsen (2006) in fluid mixtures that are contacted with adsorbents, different molecules from the fluid phase

lead to a layer between the adsorbent and the fluid that has a different concentration than the original fluid phase. They propose that this difference is the basis for the separation process. The separation process using adsorbents makes it possible for the solvent cycle to be almost at constant pressure (Madras et al., 1994). Consequently, this operation mode would be less energy consuming (Brunner & Johannsen, 2006) than traditional process as using pressure and/or temperature changes.

The adsorption-desorption process can also be used to separate compounds with similar molecular weight and polarities (Brunner & Johannsen, 2006). In vegetal matrices the extracted material is an oily mixture of which only some of its components have value-added for their properties: flavour, fragrance, colour, antioxidant properties, etc. Consequently separating these value-added components from those that do not contribute or have a negative effect on the targeted property is desirable.

Ambrogi et al. (2003) separated carotenes from natural sources by using extraction-adsorption process. Using silica gel as adsorbent they observed a selective adsorption: red pigments are captured by silica while yellow pigments stayed in the SC phase. They concluded that recovery of substances from silica gel using SC CO_2 is not an efficient process; consequently they proposed using an organic adsorbent such as cellulose.

Braida et al. (2008) concentrated bioactive (antioxidant) compounds from rosemary oleoresin. They extracted the material using organic solvents, and desorption was done using ethanol as co-solvent. They used activated carbon, active clays, silica gel, and magnesium silicate as adsorbents. Antioxidants extracted from rosemary adsorbed in activated carbon and active clays prevented oxidation of sunflower oil better than the antioxidants adsorbed in the other adsorbents. Authors concluded that the extraction-adsorption process is promising for concentrating natural antioxidant compounds.

Adsorption has been also applied to fractionate essential oils from fruits and herbs. Terpene hydrocarbons are compounds present in fruit oil that do not contribute to their fragrance or flavour, and tend to oxidize and release bad odours, while oxygen

containing compounds contribute with fragrance. Shen et al. (2002) studied the concentration of orange oil flavours by adsorbing terpene hydrocarbons into silica gel or aluminium oxide 90 that could be desorbed afterwards. They analysed changes with temperature (35-55 ºC), pressure (9.7-24.1 MPa), and CO_2 flow rate (33-67 g/min). Recovery increased with temperature (due to the increase in density), as well as decreasing flow rates (due to favoured approach to equilibrium). They concluded that it is feasible to concentrate orange oil flavour by orange oil fractionation using SC CO_2. Chouchi et al. (1996) studied bigarade peel oil fractionation. They analysed the oil recovered at different desorption times and pressures at 40 ºC. They observed three fractions: terpenic, deterpened, and residue fraction. The deterpened fraction had higher concentrations of oxygen-containing compounds than the crude oil. Reverchon & Iacuzio (1997) studied desorption of bergamot peel oil from silica gel. They observed that maximal selectivity at 40 ºC, in two steps at different pressures. At lower pressures they obtained higher concentrations of hydrocarbon terpenes; the concentration of oxygenated compounds was higher at higher temperatures. Subra et al. (1998) studied adsorption of a mixture of thirteen terpenes dissolved in SC CO_2 on silanized silica with the aim of simulating fruit peel essential oil fractionation. They achieved it modifying extraction pressure to modify the selectivity of SC CO_2.

Recovery of volatile compounds with SC adsorption also has been studied with the aim of improving coffee quality. Lucas et al. (2004) studied the adsorption isotherms of two representative components of roasted coffee aroma (ethylacetate and furfural) into activated carbon. They concluded that at higher densities, interaction forces between solute and CO_2 increases in relation to interaction between solute and activated carbon.

2.1.6 Preparative chromatography

Preparative SCF chromatography (Prep – SFC) has advantages in relation to HPLC, including the ability to change the solvent affinity to solutes, by changing conditions (pressure and temperature) (Heaton et al., 1996), the possibility of increasing productivity by increasing velocity and column loadability, and easier recovery of the compounds from the fluid phase (Guiochon & Tarafder 2011). SC CO_2-based

separations increase product concentration after the separation step, and decrease solvent as compared to HPLC-based separations (Miller, 2012). SFC is widely applied in the pharmaceutical industry for drug separation (corticosteroids and chirals). Miller (2012) concluded that the SFC might be better than HPLC in chiral separation considering selectivity, resolution, and efficiency. Miller & Potter (2008) studied preparative chromatographic resolution of racemates using HPLC and SFC. They observed that the use of SFC was effective considering time requirements. Miller (2014) studied the use of dichloromethane as co-solvent for Prep – SFC enantioseparation. He observed that dichloromethane increased productivity, solvent efficiency, and enantoselectivity. He concluded that the use of dichloromethane have a positive effect in productivity, although it have a negative environmental impact.

Regarding natural mixtures, Ramirez et al. (2007) developed a column for rosemary extract fractionation under SC conditions. They mention that, comparing with preparative liquid chromatography, some benefits of the method are fast elution time, yield improvement, product recovery by decompression, and less consumption of other solvents (generally organic solvents). They concluded that the designed column adequately meet their requirements. Ramírez et al. (2006) studied isolation of rosemary compounds using Prep-SFC. They attempted finding the optimum conditions of operation to separate compounds responsible of the antioxidant and antimicrobial activities of rosemary extract. They obtained three fractions according to elution time: the third one had higher antioxidant and antimicrobial activity than the original oil, while the first one had the essential oil.

SFC was also studied for separation of free fatty acids and triglycerides from oleic acid and sunflower oil (Škerget & Knez, 2007) using silica gel and neusilin as adsorbents. They concluded that it is feasible to separate these compounds. They also concluded that desorption can be realized with pure CO_2.

The increasing interest in diminishing the use of toxic solvents in solvent extraction, and avoid thermolabile compounds to degrade during the solute/solvent separation (commonly distillation) leaded Su et al. (2009) to study adsorption isotherms

of two fatty acid ω-3: cis-5,8,11,14,17-eicosapentaenoic acid ethyl ester and cis-4,7,10,13,16,19-docosahexaenoic acid ethyl ester on C18 bonded silica. They observed that adsorption depended highly on CO_2 density. They proposed SC chromatography as a separation alternative.

2.2 Sorption isotherms

A sorption isotherm is a function that describes the equilibrium partition of a solute between a solid matrix (adsorbent) and a solvent (in this work SC CO_2), at known conditions of pressure and temperature (Brunner & Johannsen, 2006). There has been studies of sorption isotherms mainly to concentrate compounds, such as carotenoids from paprika (Ambrogi et al., 2003), artemisin (Xing et al., 2009), ω-3 fatty acids (Su et al., 2009), salicylic acid (Kikic et al., 1996), ethyl acetate and furfural (Lucas et al., 2004), and to regenerate adsorbents (Gregorowicz, 2005). In most of those cases, the adsorbent used was silica gel, activated carbon, or clay.

To measure partition equilibrium this work uses frontal analysis. Frontal analysis is a dynamic method that measures the rupture curve (evolution with time of solute concentration in the stream leaving the column, when the stream entering the column has a constant solute concentration) at the exit of a packed column filled with the adsorbent, as a solution of the tested solute in a selected solvent at a known concentration flows through the column (Seidel-Morgenstern, 2004). The rupture curve reaches a steady state once the adsorbent is in equilibrium with the solute dissolved in the solvent and the stream leaving the column has the same concentration as the inlet stream. This process can be repeated in several stages where the concentration of the solute or solute mixture in the solvent increases progressively (cf. Appendix A).

There exist different models of sorption isotherms for a frontal analysis. Models are fitted to experimental parameters, thus sorption isotherm has to be experimentally determined for each solute-adsorbent-fluid system. Seidel-Morgenstern (2004) suggested that to know the concentration in the solid matrix, it is necesary to know the initial concentration (c_s^i) in the packed bed, its porosity (ε), the column length (L), the

superficial velocity (u), the initial concentration in the fluid (c_f^i) in cases where more than one concentration is studied in each experimet (cf. Appendix A), the concentration in the fluid (c_f), and the retention time (t_R). However, in this work, initially there is no oleoresin dissolved in the SCF nor adsorbed in the solid matrix thus, $c_s^i = 0$, and $c_f^i = 0$. Eqn. 2.1 (Seidel-Morgenstern 2004) shows how c_s is calculated. The term $\frac{L}{u}$ represents the theoretical time the fluid should take to pass through the column, or 'dead time'. Eqn. 2.1 is multiplied by a dimentionless value to convert units.

$$c_s = \frac{\left(t_R - \frac{L}{u}\right) \cdot c_f}{\frac{1-\varepsilon}{\varepsilon} \cdot \frac{L}{u}} \tag{2.1}$$

There exist several isotherms models, the simplest being a linear relation between c_f and c_s (Eqn. 2.2) that can be applied to small ranges or low concentrations (Brunner & Johannsen, 2006), where the coefficient of proportionality K is called partition coefficient (del Valle & de la Fuente, 2006)

$$c_f = K \cdot c_s \tag{2.2}$$

Non-linear sorption models include Freundlich's (Eqn. 2.3), Langmuir's (Eqn. 2.4), and Sips' or Langmuir-Freundlich's (Eqn. 2.5) equations.

$$c_f = K_F \cdot c_s^{n_F} \tag{2.3}$$

$$c_f = c_{fsat} \cdot \frac{K_L \cdot c_s}{1 + K_L \cdot c_s} \tag{2.4}$$

$$c_f = c_{fsat} \cdot \frac{K_S \cdot c_s^{n_S}}{1 + K_S \cdot c_s^{n_S}} \tag{2.5}$$

In Eqns 2.4, and 2.5, c_{fsat} represents the saturation concentration. Paramenters K and n are adjusted experimentally for each model. Subscripts of parameters K and n specify the isotherm model.

The best fitted isotherm model depends on the analyzed materials. Freundlich's equation described well the partition of PAHs between soil and SC CO_2 (Schleussinger et al., 1996). It also adjusted the partition of furfural between activated carbon and SC CO_2 (Lucas et al., 2004). Both Freundlich's and Langmuir's equations adjusted salicilic acid partition between SC CO_2 and activated carbon (Kikic et al., 1996). Langmuir's equation adjusted ethylacetate partition between SC CO_2 and activated carbon (Lucas et al., 2004). Sips' equation adjusted to valerenic acid partition between SC CO_2 and from valerian root (Salimi et al., 2008).

3. MATERIALS AND METHODS

Two types of experiments were done: one for adsorbent selection using hexane as solvent, and one of isotherm measurements using SC CO_2. Both types of experiments used as solute mixture tomato oleoresin, extracted using either hexane or SC CO_2 depending on the experiment.

3.1 Tomato oleoresin samples

Dehydrated tomatoes from Alto la Cruz (Santiago, Chile) were complimentary dried in a WTB Binder (Binder, Tuttlingen, Germany) convection oven at 60 ºC for 5 days (final moisture content 13%), pelletized in a Pellet Pros PP85 (Dubuque, IA) device with 4-mm openings (pellets of ~10 mm length), milled in a food processor Moulinex (Barcelona, Spain), and size classified to recover a coarse (+35 mesh) fraction. The pretreatment has several aims, including fracturing cell walls, reducing particle size, and removing dust particles to facilitate subsequent oleoresin extraction without operational problems such as caking, screen blinding, and water co-extraction. The resulting material was placed in a sealed bag and held at 4 ºC in a refrigerator up to analysis.

Pretreated tomato samples were extracted in 100 cm^3 Schott flasks using technical grade hexane (Heyn, Santiago, Chile) at 55 ºC in a convection oven in food-grade nitrogen atmosphere (N_2, Indura S.A., Santiago, Chile). Hexane was replaced every hour and extraction was continued up to exhausting the substrate (*i.e.,* colourless mixture). Extract samples were pooled and hexane was removed from tomato oleoresin by vacuum evaporation (0.05 Pa absolute pressure) in a Büchi (Flawil, Swiss) rotary evaporator. This hexane-extracted oleoresin was placed in a 100 cm^3 Schott flask in a N_2 atmosphere and held at -18 ºC in a freezer up to analysis.

Pretreated tomato samples were also extracted with SC CO_2 using the method of Germain et al. (2005). Extractions were carried out using food-grade CO_2 (Indura S.A., Santiago, Chile) in a computer-controlled Thar Technologies' (Pittsburgh, PA) SFE-1L unit, equipped with a Coriolis flowmeter (CMF010M324NU, Micro Motion, Boulder, CO), a P-200A-2 pump, a 1-LT-PH extraction vessel (1000-cm^3 capacity), a ABPR-200-

2 back pressure regulator (BPR), a CS-200-cm^3 cyclone separator (200 cm^3 capacity), and a CO_2 recycling system from Eurotechnica (Bargteheide, Germany). The mass flow rate of CO_2 (150 g/min) was adjusted by the pump (variable speed), the extraction temperature (55 ºC ± 2 ºC) was adjusted by circulating water from a PolyScience 8205 (Niles, IL) bath through the jacket of the extraction vessel, and the extraction pressure (45 MPa ± 2 MPa) was controlled by the BPR. Extractions were extended for 9 h, and tomato oleoresin was collected from the cyclone in a 10 cm^3 amber vial. This SC CO_2-extracted oleoresin was placed in a sealed 10 amber vial with a N_2 atmosphere that was held at -18 ºC in a freezer up to analysis.

3.2 Adsorbent selection

Adsorbents were selected by measuring the equilibrium partition of hexane-extracted tomato oleoresin between the adsorbents and hexane at 40 ºC using the method of Chu et al. (2004a, b, c). Studied adsorbents were activated carbon, microcrystalline cellulose, and silica gel from Merck (Darmstadt, Germany), celite from Sigma Aldrich (St. Louis, MO), and chitosan in microspheres kindly provided by Foodomics CIAL (Madrid, Spain) (Díez-Municio et al., 2011) (Table 3.1). Gravimetric methods were used for bulk density estimation.

In adsorption experiments, 100 cm^3 Schott flasks were loaded with 100 cm^3 of analytical-grade hexane (Heyn, Santiago, Chile), together with a known amount of hexane-extracted oleoresin, 1 cm^3 of different adsorbents (accurately weighed), and 3 mm glass beads to prevent adsorbent settling. Control flasks were prepared similarly, but without adsorbent. The amount of oleoresin added was such that its initial concentration in hexane was approximately 0.20, 0.30, 0.50, 0.80, 1.00, or 1.50 mg/cm^3. N_2 gas was used to displace headspace air before closing the flasks to avoid oleoresin oxidation during equilibration. Flasks were placed in a JSR JSSI-100C rotary incubator (Gongju, Korea) set at 40 ºC and 180 rpm. Rotary shaking and glass beads prevented the adsorbent from settling in the flask during experiments. Aliquots of the hexane-phase

were sampled during experiments and analysed as described below. All experiments were performed in triplicate.

Table 3.1: Characterization of the adsorbents considered in this work: particle diameter and bulk density for activated carbon, microcrystalline cellulose, celite, silica gel, and chitosan in microspheres

	Particle diameter (μm)	Bulk density (kg/m^3)
Activated carbon	< 100[a]	372
Microcriystaliline cellulose	20 – 160[b]	414
Celite	≥ 45	346
Silica gel	63 - 200	460
Chitosan in Microspheres	1000 – 2000	410

[a] Providers assure that 90% of the product meets this characteristic.

[b] Providers assure that at least 80% of the product meets this characteristic

Following homogenization of flask contents, a 1.5 cm^3 aliquot was sampled using a micropipette (Gilson pipeteman G P1000G, Middleton, WI), placed in 1.5-cm^3 Eppendorf tubes, and centrifuged at 6000 rpm in a TOMY HF120 (Palo Alto, CA) apparatus to precipitate out the adsorbent particles sampled. Clarified liquid from Eppendorf tubes was sampled with the micropipette and analysed in a UV-mini 1240 (Shimadzu, Kyoto, Japan) spectrophotometer to estimate the oleoresin content using a calibration curve.

The calibration curve was constructed using the control flasks and 6 concentrations to make sure that spectrophotometer's readings were consistent with each mixture concentration. Samples from all flasks (control and adsorbent) were diluted with

analytical-grade hexane in 1:3 or 2:3 dilutions to meet the spectrophotometer volume requirements, and subsequently readings were multiplied by the dilution factor (3.0 or 1.5, respectively). The wavelength used was chosen by scanning oleoresin absorption in hexane (466 nm or 469 nm depending on the oleoresin batch). Concentration in the adsorbent was calculated with Eqn. 3.1 (Ahmad et al., 2009; Choong et al., 2010)

$$c_{s,t} = \frac{V \cdot (c_{l,0} - c_{l,t})}{W}, \tag{3.1}$$

where, $c_{s,t}$ represents the concentration of oleoresin in the adsorbent (mg/g); V, the volume of the mixture (100 cm^3); $c_{l,0}$, the original concentration of the mixture (mg/L); $c_{l,t}$, the concentration of the mixture (mg/L) at time t; and W, the adsorbent weight (g).

3.3 Adsorbent assessment

For the selected adsorbents, the equilibrium partition of SC CO_2-extracted tomato oleoresin was measured between them and SC CO_2 at 40 ºC and 28 MPa using frontal analysis. Fig. 3.1 shows the equipment in which these experiments were carried out. Desorption was also analysed using frontal analysis, by decreasing the concentration of the solute or solute mixture in the solvent progressively.

The equipment used in these experiments is a two-part system. In one subsystem, SC CO_2 at a selected temperature and pressure gets saturated with the oleoresin that is loaded in a 40-cm^3 high-pressure cell (6 in Fig. 3.1) placed horizontally, by recirculating the SC CO_2 phase through the equilibration loop (5, 6, 7, and 8) with a high-presssure gear pump (5) (Micropump GAH-T23, Vancouver, WA) powered by an external motor (Siemens Micromaster 411, Congleton, UK). This equilibration subsystem is interfaced through an automated injection valve (7) with a flow-through (dynamic) subsystem. In the dynamic subsystem, SC CO_2 at working conditions is pumped at a controlled flow rate by a high-pressure positive displacement pump (9) (Jasco PU-2086 Plus,Tokyo, Japan) through a packed bed column (0.7-cm inner diameter, 30-cm length) (11). The automatic injection valve (Jasco HV-2080-01, Tokyo, Japan) is operated with a timing relay (Siemens LOGO 230RC, Munich, Germany); the size of the injection loop (50 μL) and time between pulses (off-on, on-off) determines the relative proportions of

oleoresin-saturated SC CO_2 and pure SC CO_2 fed to the packed bed column. From the standpoint of the equililibration subsystem, the injection valve replaces 50 μL of oleoresin-saturated SC CO_2 by 50 μL of pure SC CO_2 at the same conditions, and this places the limits to the relay time and the length of the experiment, that are related to the disolution rate and amount of tomato oleoresin in the equilibrium cell. The equilibration and dynamic subsystems are placed in a single thermostated air bath equipped with a hot-air blower (Leister Hotwind S, Sarnen, Switzerland) for heating, and a controller (Hillesheim HT42-10P, Waghäusel, Germany) for temperature control. The pressure of the dynamic subsystem is controlled by an automatized back-pressure regulator (13) (Jasco BP-2080 Plus, Tokyo, Japan). The stream leaving the column of the dynamic subsystem flows through a high-pressure UV-Vis detector (12) (Agilent G1214A, Santa Clara, CA) that measures its absorbance (oleoresin concentration) and it is controlled by a digital interface (Jasco LC-NET II/ADC, Tokyo, Japan) equipped with a data analysis software (Jasco ChromPass Chromatography Data System ver. 1.7.403.1, Tokyo, Japan). The column of the dynamic subsystem was packed with either 500-μm glass beads or a 500-μm glass beads with a top layer (0.1-5 cm thick) of a selected adsorbent. Experiments with the column filled with glass beads allowed determining a calibration curve of olerosein concentration *versus* relay time. The bottom layer of glass beads in the columns with adsorbent allowed homogenizing the oleoresin concentration in the stream entering the adsorbent layer (SC CO_2 up-flowed through the column).

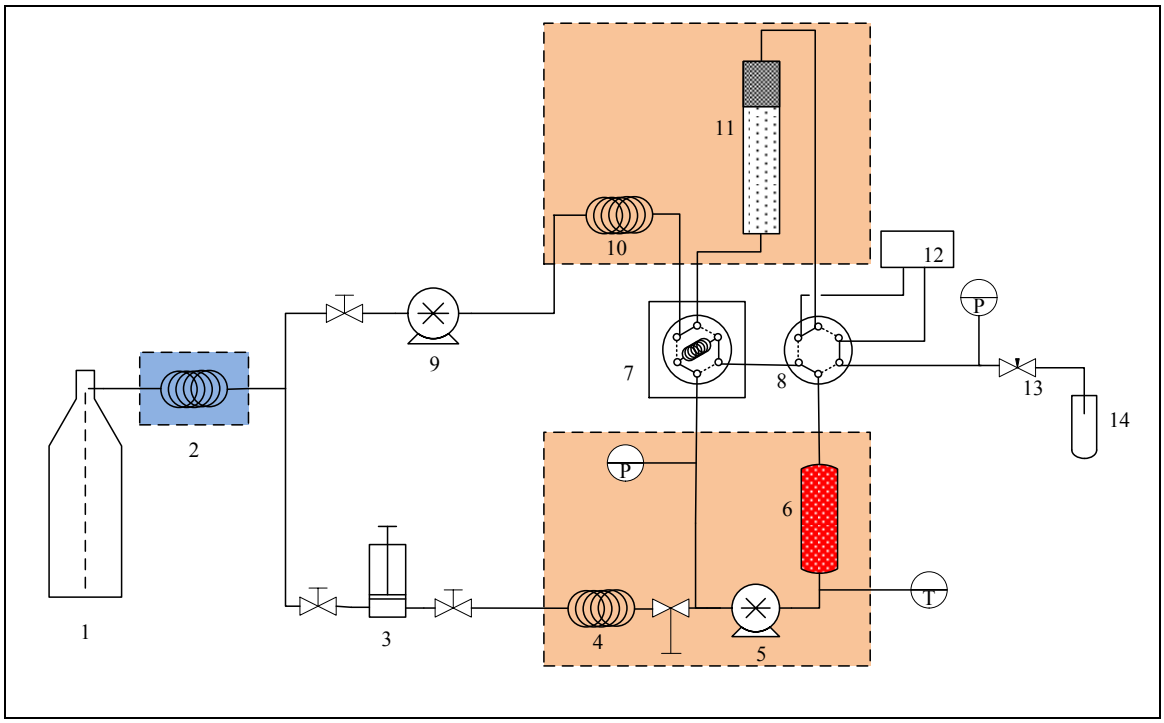

Figure 3.1: Isotherm measurement equipment. Orange areas represent heated zones, and blue areas represent cooled zones. (1) CO_2 cylinder, (2) cooling bath, (3) syringe pump, (4, 10) heating coils, (5) recirculation pump, (6) high pressure cell, (7) automatic 6-way valve, (8) 6-way valve, (9) positive displacement pump, (11) packed bed column, (12) spectrophotometer, (13) automatized back-pressure regulator, and (14) vial.

Initially the air bath was set at the desired temperature (40 ºC), the equilibrion cell was filled with 3-mm glass beads and loaded with 3-6 g of oleoresin (according to equilibration subsystems volume, and oleoresin density). The equilibration subsystem was loaded with SC CO_2 at the desired pressure (28 MPa) using a syringe pump (Teledyne Isco 260 D, Lincoln, NE). After isolating the equilibrium subsystem, the high-pressure gear pump was set to 30 Hz (~ 40 cm^3/min, performance using distilled water is considered) and turned on. Following overnight equilibration, saturation was measured as follows. Oleoresin-saturated SC CO_2 was sampled in an open loop mode (syring pump operating in a pressure controlled mode). To ensure a representative

sample amount, expanded volume of CO_2 was < 2 L. The sample was collected in 50 cm^3 sampling tube, and weighed in an electronic balance Sartorius PRACTUM224-1S (Göttingen, Germany). The expanded CO_2 was measured in a drum-type flowmeter (Ritter TG-05/5, Bochum, Germany). The saturation concentration of oleoresin in SC CO_2 was estimated as grams of oleoresin per liter of CO_2.

In a second stage, the dynamic subsystem with the column packed with one of the aforementioned materials was equilibrated using 2.6 cm^3/min (estimated measuring the expanded flow of CO_2 in the flowmeter) of pure SC CO_2 at 40 ºC and 28 MPa. Following equilibration, the automatic injection valve was started with a set relay time. The absorbance of the SC CO_2 stream leaving the subsystem was measured the in the UV-Vis apparatus set at a wavelength of 486 nm. Two types of experiments were performed. Firstly, several short (30 s) pulses with variable (increasing) solute concentration were applied to obtain a near-Gaussian peaks at the detector. Secondly, several step pulses with variable (increasing) concentration were maintained up to obtaining the rupture curve (concentration of tomato oleoresin in the SC CO_2 stream leaving the dynamic subsystem as a function of time) up to reaching a plateau where the absorbance was as expected from the calibration curve as a function of the selected relay time. The rupture curve for desorption was also recorded from the time where the switching valve was turned off and the dynamic subsytem was fed with pure SC CO_2 up to the time where the absorbance reading went back to zero, as expected.

Time between two saturated pulses determined the concentration of the final current. Pulse duration was 1.5 s that would empty the 50 μL loop at the selected SC CO_2 feed rate. Time between pulses were 2.5, 3, 4, 5, 7, and 10.5 s, thus cycle times were 4, 4.5, 5.5, 6.5, 8.5, and 12 s. Stream concentration was estimated considering the saturation concentration of tomato oleoresin in SC CO_2 and the ratio of loop volume and the total volume that flows through one cross section during the cycle time. Concentrations at this cycle times were of 28, 25, 21, 18, 13, and 9% of saturation concentration, respectively. A calibration curve was constructed using the column from the dynamic system filled with glass beads, and using all 6 cycle times.

Gravimetric methods were used to measure oleoresin density. Porosity was estimated using Benyahia & O'Neill (2005), and Dixon (1988) equations (shown in Appendix B). The volume of equilibration subsystem was measured by filling it with SC CO_2 at known conditions and emptying it at atmospheric conditions. Volume of expanded CO_2 was measured in the flowmeter.

3.4 Statistical analysis

An ANOVA statistical analysis was conducted among adsorbent selection samples, using StatPlus software (AnalystSoft Inc., Alexandria, VA). Spectrophotometer readings from samples taken from one adsorbent flask at certain oleoresin concentration were compared with readings from samples from their respective control flasks.

4. RESULTS AND DISCUSSION

4.1 Adsorbent selection

The concentration of carotenoids in tomato oleoresin samples extracted with hexane varied between batches due to differences in the substrate (different storage times before extraction), amount of hexane used in extracting, and/or extent of hexane removal from the oleoresins during rotary evaporation. In any case what was important was the actual concentration used in adsorption experiments, which was adjusted by diluting with added hexane. In all cases, as shown in Fig. 4.1 calibration curves of concentration *versus* absorbance exhibited linear behaviour (slope = 0.0012 and R^2 = 0.99338), and they were used to relate absorbance and oleoresin concentration in batch adsorption experiments.

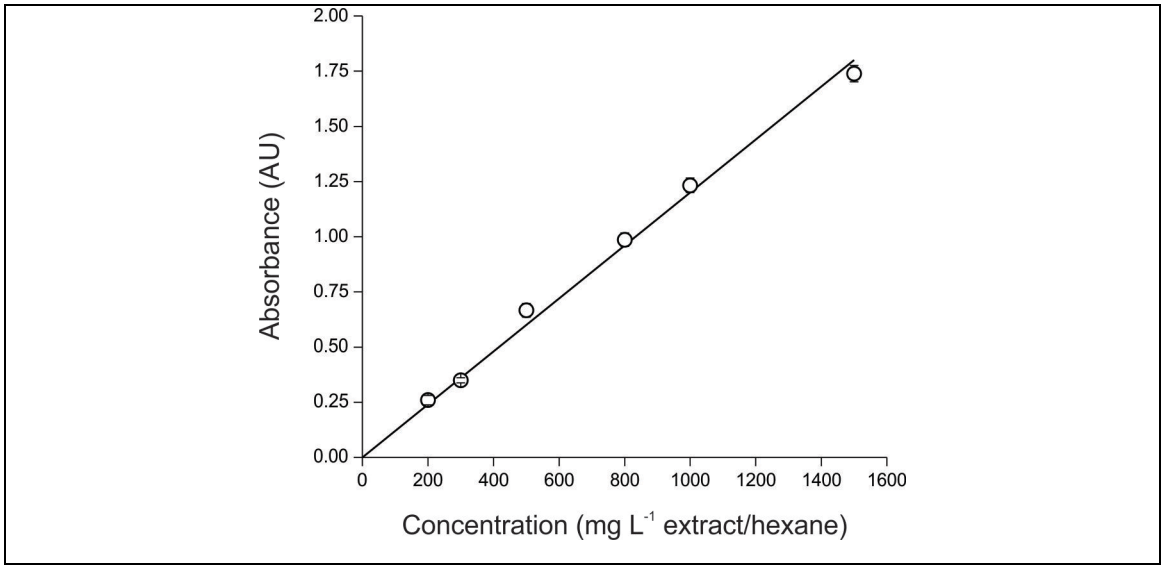

Figure 4.1: Spectrophotometer response for samples at different tomato oleoresin concentrations in hexane.

Absorbance readings were normalized by the initial reading (done before adding the adsorbent) and treated as percentages of it, to account for small differences in initial

concentration between flasks and to make different concentrations comparable. Control samples were normalized regarding their average measurement for each concentration.

Figure 4.2 show the differences in adsorption between adsorbents when having the same concentration of tomato oleoresin in hexane. Similar trends were observed when changing oleoresin concentration. Activated carbon fully adsorbed tomato oleoresin in a very short time (time scale shorter than experimentally assessed). Silica gel adsorbed tomato oleoresin fast, however adsorption was only partial and was completed in a larger time scale than in the case of activated carbon. Both cellulose and celite did not absorb tomato oleoresin, and differences in absorbance of the solvent phase did not change during experiments more than observed for control flasks without adsorbent. Chitosan showed an intermediate behaviour in that the adsorption was only partial, and of limited extent.

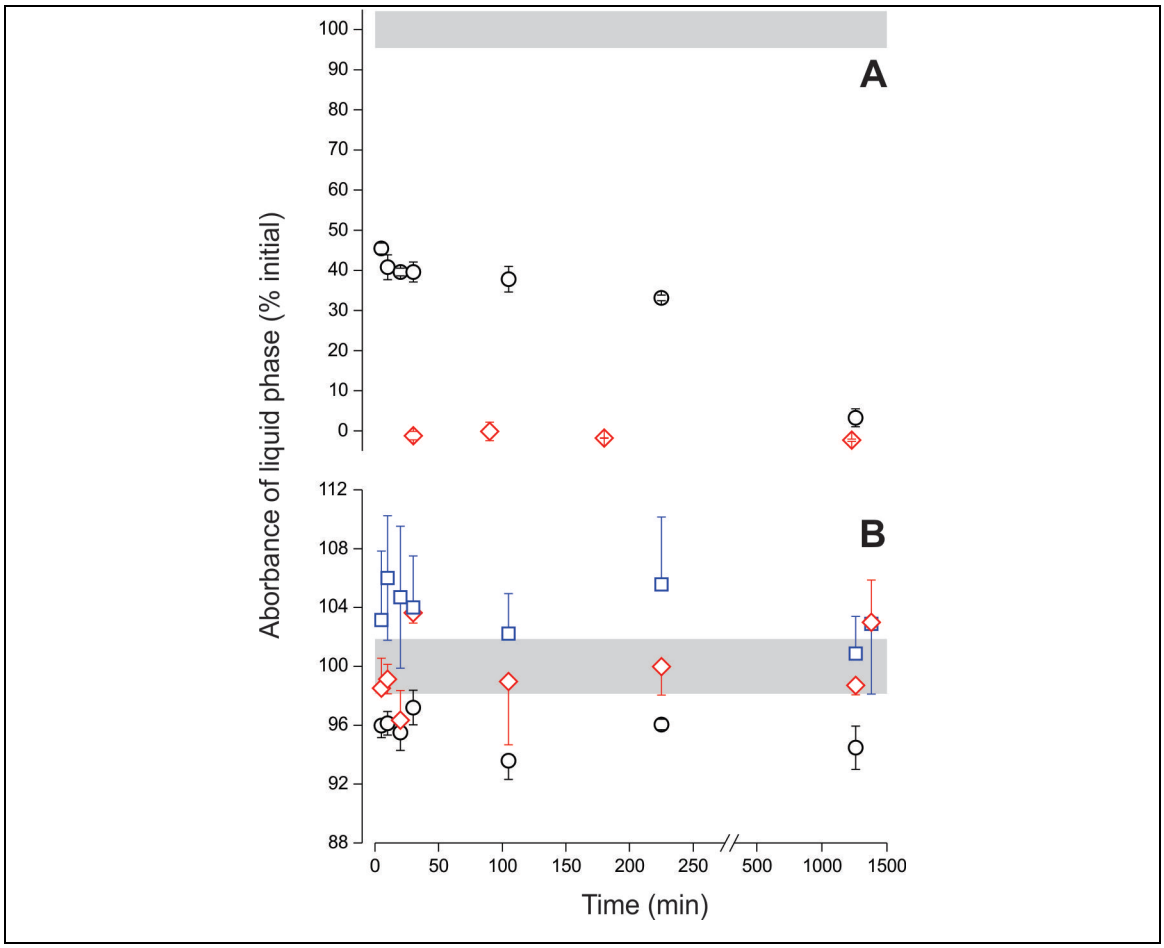

Figure 4.2: Spectrophotometer response for samples with different adsorbents. (**A**) Activated carbon (◇) and silica gel (○) using an initial concentration of 800 mg L^{-1} extract/hexane. (**B**) Microcrystalline cellulose (□), celite (◇), and chitosan in microspheres (○) using an initial concentration of 1000 mg L^{-1}. Grey areas represent the standard deviation of control samples.

Statistical analysis showed significant differences in percentage of adsorption in chitosan as compared to its control ($F = 31.09 > F\ critical = 6.67$ at $\alpha = 0.02$), whereas cellulose and celite samples did not. The differences between samples, is qualitatively illustrated by photographs taken following >48 h of equilibration (Fig. 4.3). Activated carbon was discarded for interacting too strongly with tomato oleoresin. Celite and

cellulose were discarded for interacting too weakly with tomato oleoresin. The selected adsorbents were silica gel and chitosan in microspheres.

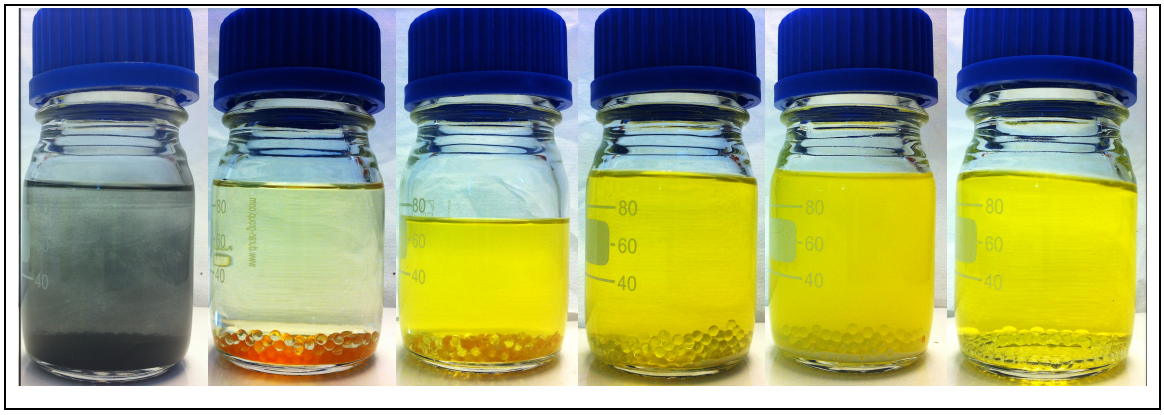

Figure 4.3: Visual comparison of adsorbents. From left to right: activated carbon, silica gel, chitosan in microspheres, microcrystalline cellulose, celite, and control.

Using Eqn. 3.1 it was possible to calculate that chitosan adsorbed up from to 38 ± 4 mg/g oleoresin/chitosan from a mixture containing 145 mg/L (original concentration of 200 mg/L) oleoresin/hexane, to 76 ± 21 mg/g from a mixture containing 846 mg/L oleoresin/hexane (original concentration of 1000 mg/L, Fig. 4.4). On the other hand, silica gel absorbed up to 432 ± 10 mg/g oleoresin/silica gel (all oleoresin available) when equilibrated with a mixture containing initially up to 1500 mg/L oleoresin/hexane.

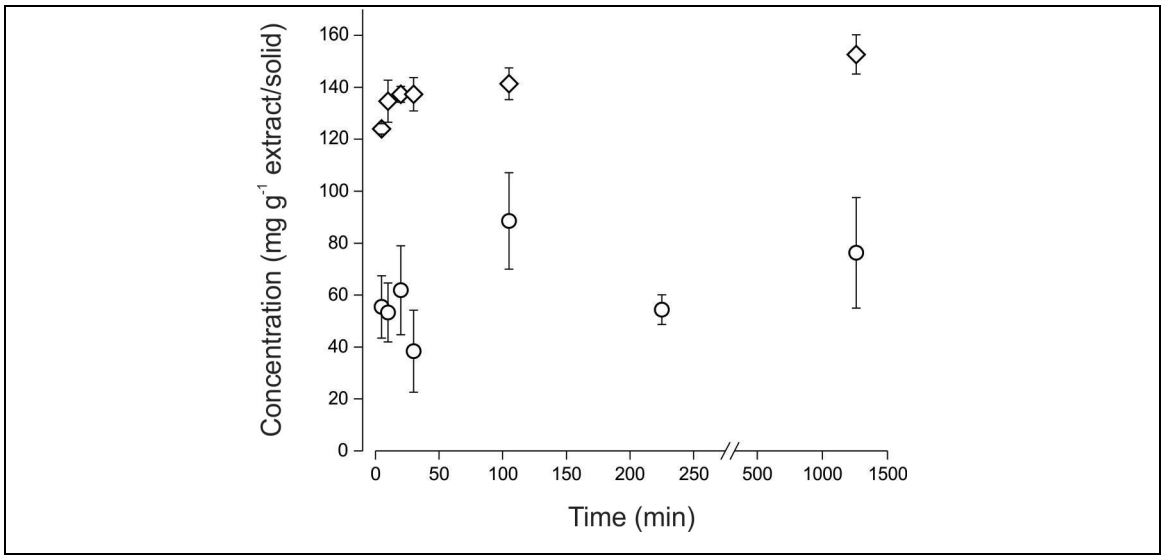

Figure 4.4: Tomato oleoresin concentration in chitosan in microspheres (○) (original oleoresin concentration: 1000 mg L^{-1}) and silica gel (◇) (original oleoresin concentration: 800 mg L^{-1}).

4.2 Sorption isotherm

The SC CO_2 in the 50 μL loop in the automated valve (7 in Fig. 3.1) has to be kept saturated with tomato oleoresin during the whole experiment. The equilibration cell can be loaded with < 40% of its free volume with oleoresin, because of its horizontal position. Considering $\varepsilon = 0.425$, available volume of the equilibrium cell is of 17 cm^3. Tomato oleoresin density is 0.94 g/cm^3 thus oleoresin should not occupy more than 6.8 cm^3, and weight 6.4 g. Since SC CO_2 saturation concentration with tomato oleoresin was of 8.52 g/L (9.48 g/kg), at least 0.28 g of oleoresin in the equilibration cell were necessary to saturate the 33 cm^3 of CO_2 available in the static system.

The absorbance reading in the stream leaving the column ranged from 35 AU for 9% saturation to 95 AU for 28% saturation, in calibration curves (Fig. 4.5A for adsorption, and Fig. 4.5B for desorption). The UV-Vis response was lineal and proportional (slope = 39.879 and $R^2 = 0.99821$), as expected (Fig 4.6). Results from this part show that 30 cm of packed glass beads are enough to homogenize the SC CO_2

stream produced with the injection method, and that 'dead time' calculated for this equipment is 130 s (time that takes to reach half of the maximum absorbance), thus the free volume of the dynamic subsystem between the automatic valve to the UV-Vis is 5.73 cm^3.

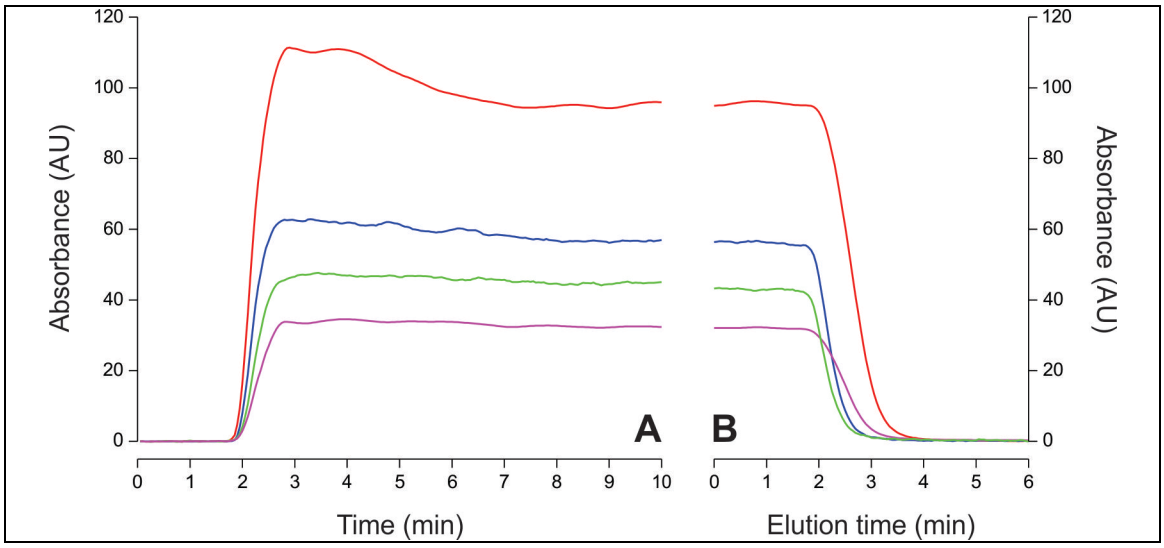

Figure 4.5: UV-Vis response to different oleoresin concentrations (as percentages of the saturation concentration) in SC CO_2, with column filled with glass beads: **A** breakthrough curve and **B** desorption curve. Red, blue, green and magenta lines represents 28, 18, 13 and 9% of saturation concentration respectively.

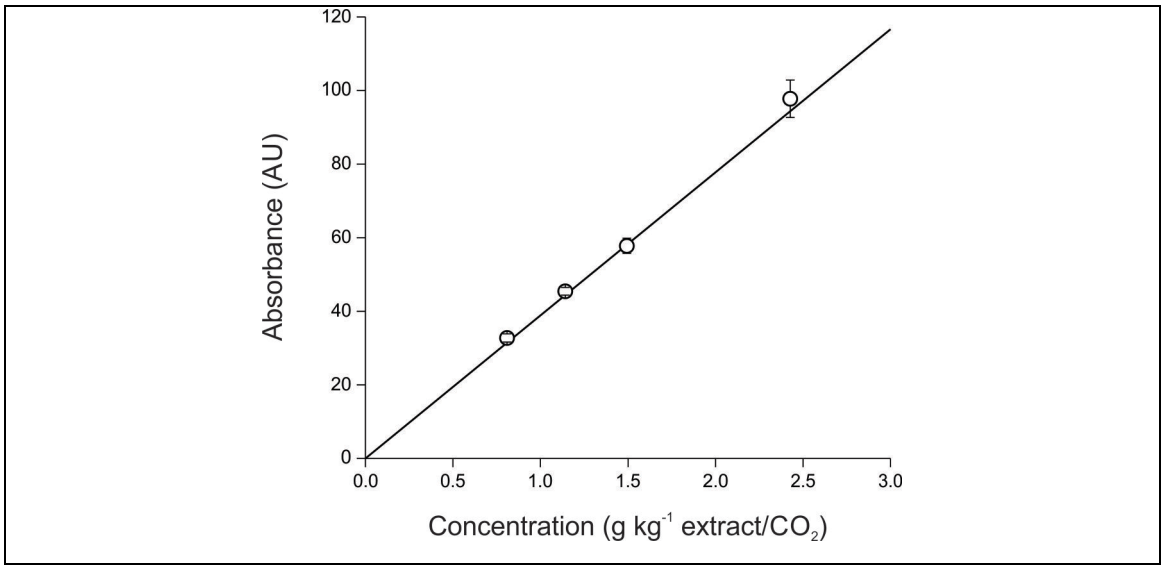

Figure 4.6: Relation between oleoresin concentration in the SC phase, and UV-Vis response.

The same experiment (13%) was run in triplicate to test reproducibility. Figure 4.7 shows that the three curves behave similarly although they have small differences (their average and maximum standard deviation are 1.6 and 2.2 AU respectively).

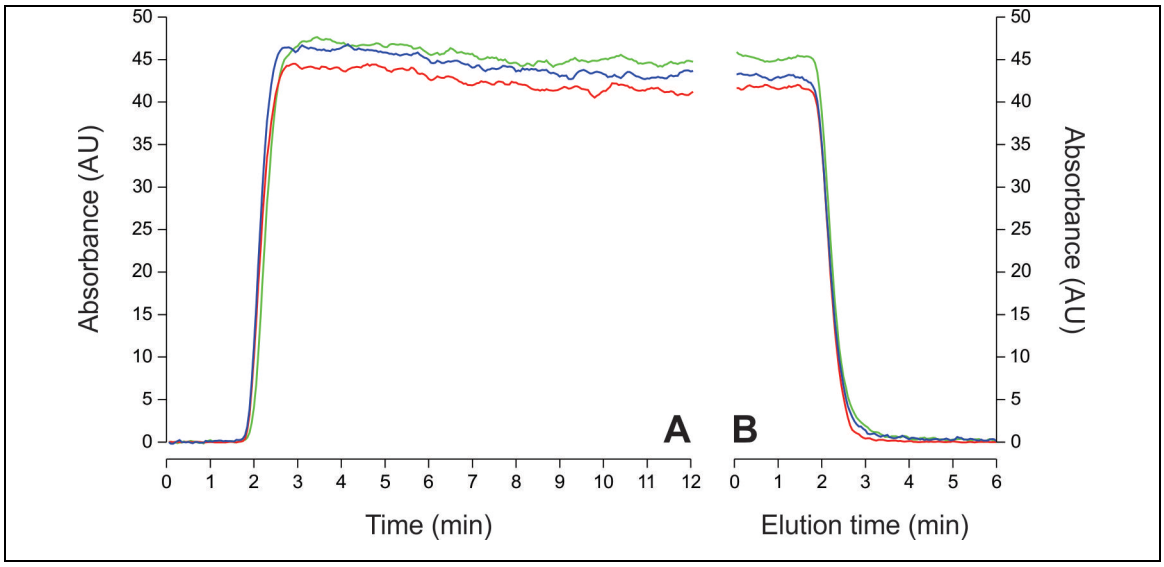

Figure 4.7: Reproducibility of calibration curve assessing by running the experiment using 13% of saturation concentration in triplicate. **A** breakthrough curve and **B** desorption curve.

A standard calibration curve is shown in Fig. 4.8. It was build by the combination of all calibration curves, making sure that their UV-Vis average reading between the maximum and the minimum was achieved at the previously calculated dead time. This curve can be used to compare results from adsorbents experiments at different concentration only by modifying its maximum.

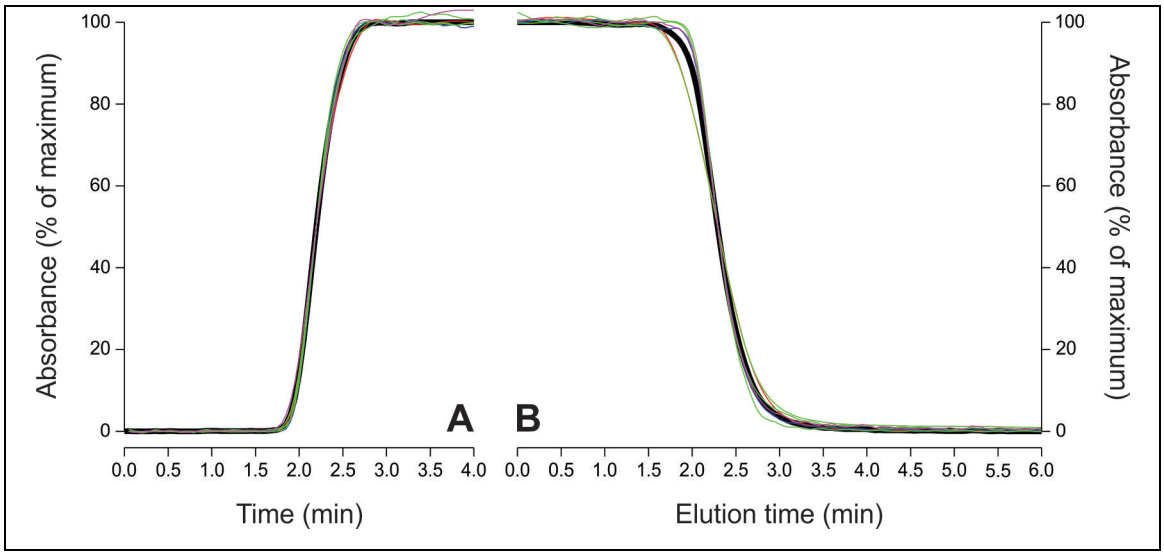

Figure 4.8: Standard calibration curve (black). Red, blue, green and magenta lines represents 28, 18, 13 and 9% of saturation concentration respectively. **A** breakthrough curve and **B** desorption curve.

Spectrophotometer readings using a top layer of 1 mm of silica gel, at 28% of saturation in the dynamic subsystem column are shown in Fig. 4.9. The adsorption capacity of silica gel is large, even for a very small sample; this impedes the stream leaving the column from reaching the concentration defined by the set relay time. Equilibration cell was loaded with 5.5 g of tomato oleoresin, and during the 170 min that the 28% saturation concentration (6.4 g/L for this batch of oleoresin) the experiment lasted, 0.8 g of oleoresin were used. The observed behaviour was attributed to the high affinity that silica gel has to tomato oleoresin. It could also lead to problems related with demands for the re-saturation process and/or time required to fully desorb the oleoresin from the adsorbent as observed by Ambrogi et al. (2003). Further studies could consider using much less silica gel in the column; this was impossible using the column of this work because its diameter was too large to ensure an homogeneous adsorbent packing. For example a lower diameter column could be used, but this might place restrictions to the selected pump.

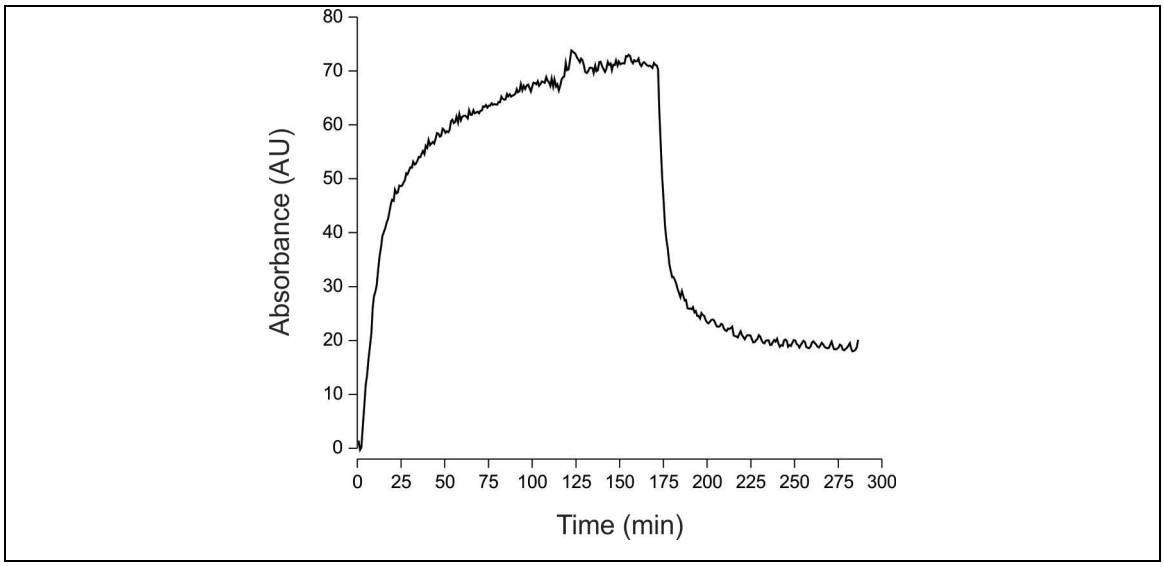

Figure 4.9: UV-Vis response to tomato oleoresin 28% saturation concentration in SC CO_2, with column filled with 1 mm of silica gel.

A 5 cm top layer of chitosan was packed in the dynamic subsystem column to analyse the partition equilibrium of tomato oleoresin between chitosan in microspheres and SC CO_2. Short (30 s) pulses of 28, 25, 21, 18, 13, and 9% saturation concentration were applied to the column filled with chitosan before and after analysing breakthrough curves. The UV-Vis responses varied for 9% concentration as shown in Fig. 4.10. Fig. 4.10A shows large differences in the response of detector between replicates done in the first set of experiments in favour of the second one that is consistent with a large amount of tomato oleoresin being retained by chitosan in the first replicate, whereas Fig. 4.10B shows very small and random differences in the same response between replicates done in the second set of experiments. There is clearly less tomato oleoresin being adsorbed by chitosan in the second than in the first set. These results are consistent with irreversible adsorption of tomato oleoresin in chitosan, and without differences in the irreversibly adsorbed amount at the time where the second set of experiments were carried out. This has been observed before, for the regeneration of activated carbon, where adsorption capacity decreased after the first adsorption-desorption cycle, but it remained stable afterwards (Tan & Liou 1989b). Figure 4.11 shows pictorial evidence of

this irreversible adsorption as a reddish tinge of chitosan microspheres packed in the column. Consistent with this hypothesis of irreversible adsorption, there were also differences in breakthrough curves between the first and second set of experiments, which were reproducible only the second time.

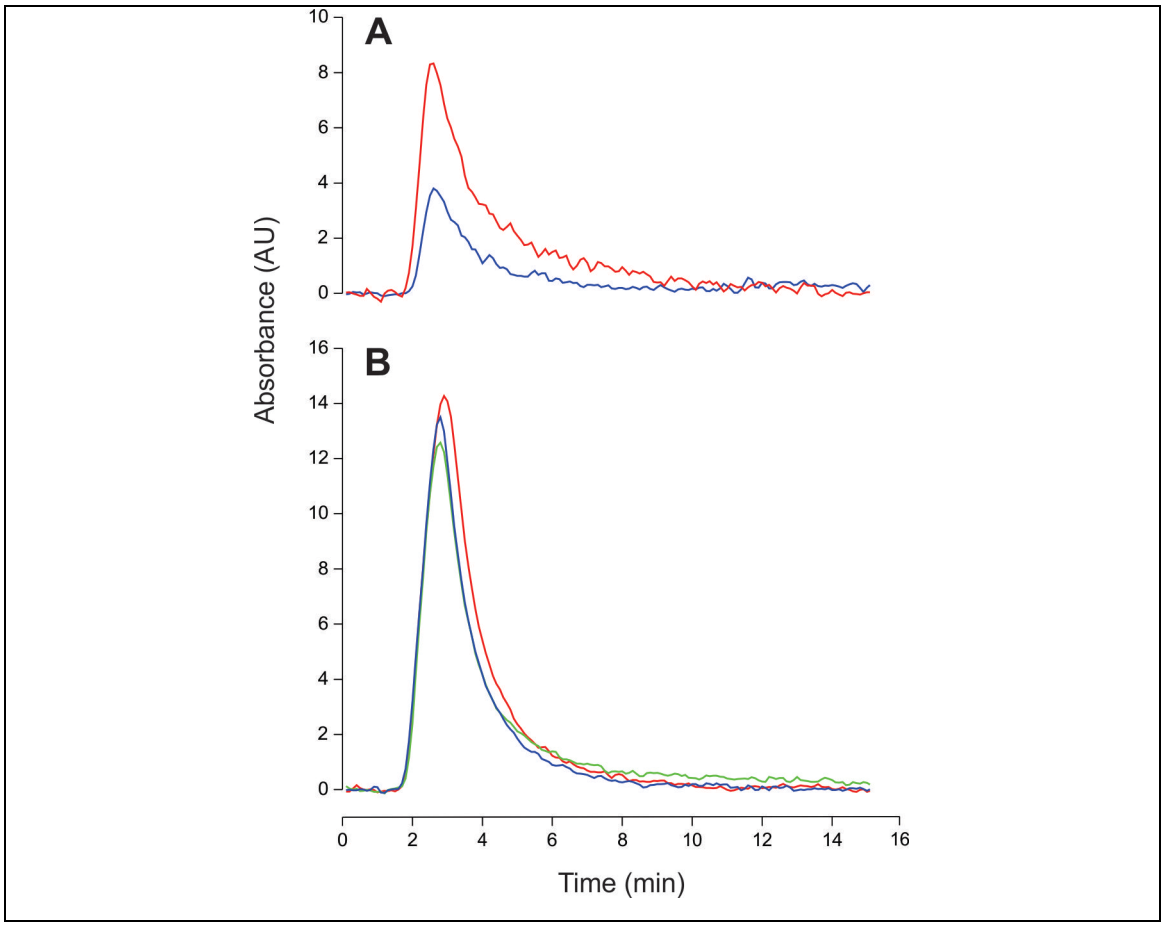

Figure 4.10: Reproducibility of adsorbent experiments. **A** Pulses of 9% saturation concentration in a column filled with 5 cm of chitosan in microspheres before breakthrough curves. Blue and red lines represent the first and last repetition respectively. **B** Repetition of reproducibility experiment after breakthrough curves.

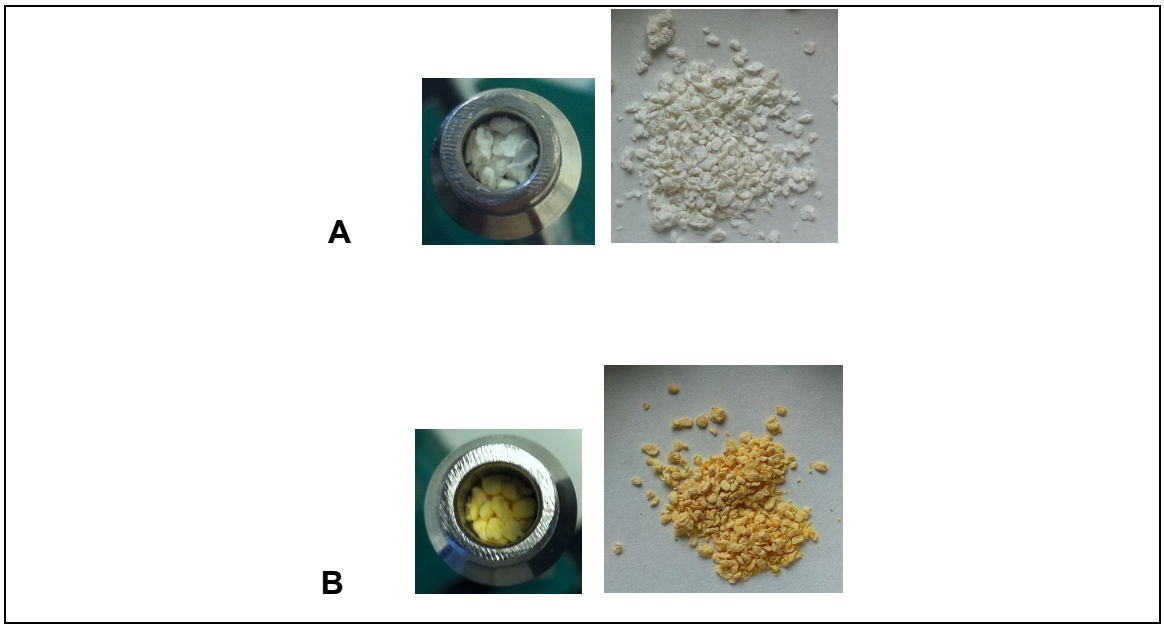

Figure 4.11: Chitosan packed bed before **A** and after **B** the breakthrough curves experiments.

In Figure 12 the black lines represent breakthrough curves for the sorption stage (when changing from pure SC CO_2 to SC CO_2 partially saturated with tomato oleoresin, left) and desorption stage (when changing from SC CO_2 partially saturated with tomato oleoresin to pure SC CO_2, right) for experiments done using the glass-bead column with a 5 cm top layer of chitosan. These curves were roughly as expected. Unlike the case of the column filled with glass beads, breakthrough curves did not exhibit an initial shoulder; furthermore, they showed a tendency to increase rather than decrease with time in the plateau region, which may signal slow sorption by chitosan in this period, or fractionation of the oleoresin by chitosan. The equilibrium oleoresin concentration in the chitosan layer was estimated both for sorption and desorption using the two methods explained below.

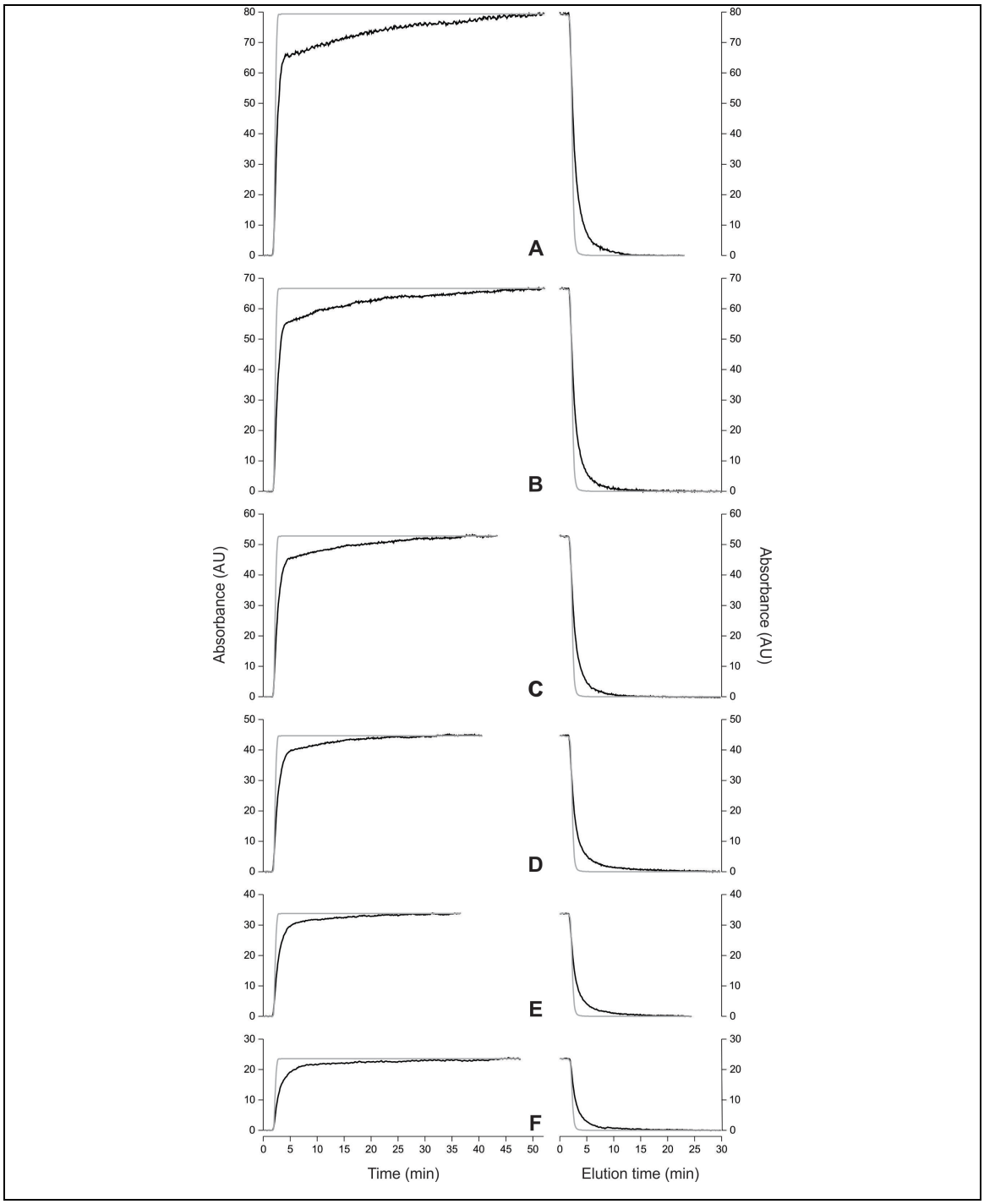

Figure 4.12: UV-Vis response with chitosan in microspheres (black) together with their standard calibration curve (grey): **A**, **B**, **C**, **D**, **E**, and **F** represents 28, 25, 21, 18, 13, and 9% of saturation concentration. Breakthrough curves (right) and desorption curves (left).

The first method is based on mass balances. Figure 4.12 shows breakthrough curves for the sorption stage and desorption stage (black lines) as a function of extract concentration, together with their respective standard calibration curves (grey lines). The area between the two curves in the sorption stage (figures on the left) represents the amount of tomato oleoresin held by chitosan that does not leave the column (or the total amount of adsorbed tomato oleoresin), whereas the area between the two curves in the desorption stage (figures on the right) represents the weight of tomato oleoresin released by the chitosan to the stream of SC CO_2. To do this the curves for the glass bead column were extended. The amount of oleoresin adsorbed was estimated by multiplying difference in area between both curves (treated as proportion) to the total amount of oleoresin that came out during the experiment.

The second method used data in Figure 4.12 to estimate the amount of adsorbed (breakthrough curve) or desorbed (elusion curve) tomato oleoresin based on the increase in residence time of the mixture as compared to a system without any chitosan using Eqn. 2.1. This residence time can be estimated as those times noted in Figure 4.5 where solute concentration reached one half of the initial concentration. Dimensionless value to correct units from Eqn 2.1 was calculated, $c_{f_{sat}}$ considered was 8.52 g/L, and packed bed porosity was estimated assuming chitosan as 1.5 mm diameter spheres.

For this estimate to be precise, a nearly step change in absorbance is required and it was not always obtained (although the slope of the curve of absorbance versus time was always very steep). The four estimated values of solid concentration for each fluid concentration should ideally coincide, but this was not the case as summarized in Figure 4.13. Independent on the method, the values for adsorption did not coincide with those for desorption, suggesting methodological errors or hysteresis of sorption phenomena. Hysteresis may occur between intermediate oleoresin concentrations in the SC CO_2 but not when there is no oleoresin in SC CO_2 at the end, and when the effects of irreversible adsorption have been discarded by pretreating chitosan with tomato oleoresin, as attested in Fig. 4.10. The method based on breakthrough curves is very imprecise. This is due mainly to axial dispersion that was large considering the poor packing of large chitosan

microspheres, and the fractionation of extract that might occur during experiments. Mass balances, on the other hand are complicated due to changes in absorbance with time during equilibration, there might be difficulties in keeping the SC CO_2 phase saturated when using large percentages of saturation, thus shoulders in curves using glass beads appears. From the results obtained, it is better to apply the method based on mass balances if fractionation is observed, as in the case of a multicomponent mixture such as tomato oleoresin.

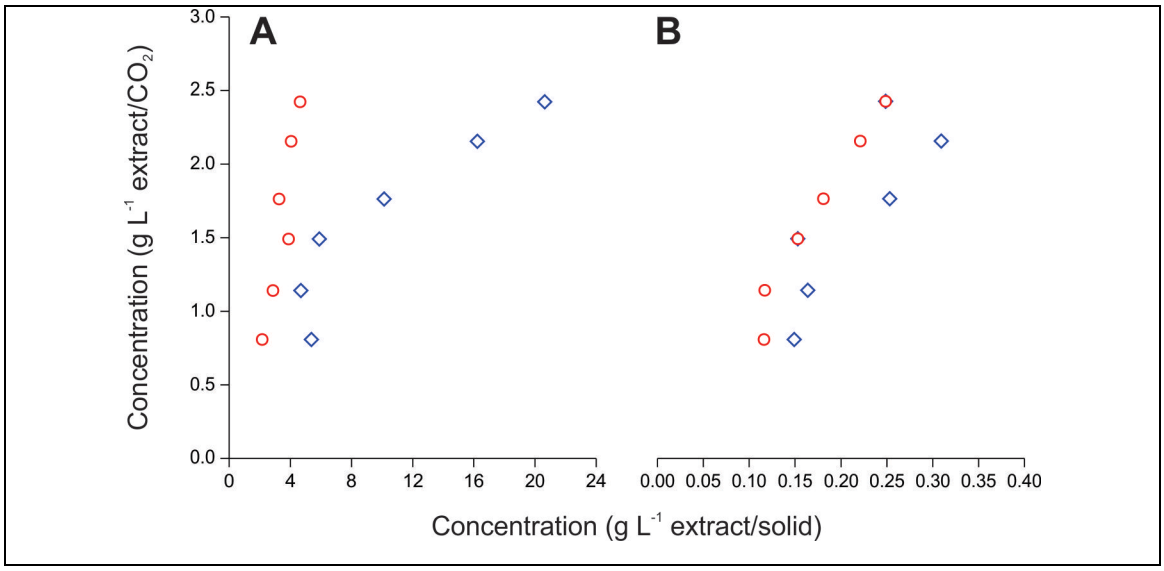

Figure 4.13: Oleoresin concentration in solid and fluid phases: **A** Concentration calculated with mass balance method, and **B** Concentration calculated with breakthrough curves method. Adsorption (◇) and desorption (○).

Four isotherm models were adjusted to both analysis methods: linear, Freundlich, Langmuir, and Sips (all of which are introduced in section 2.2). Parameter optimization was done in MATLAB. Parameters found are summarized in Table 4.1, and the best and worst fitted isotherms for each case are shown in Figure 4.14. Results show that the interaction between tomato oleoresin and chitosan in microspheres is low, even though chitosan in microspheres do adsorb oleoresin. When using the first method Freundlich's

and Sips' models behave similarly in the working range of concentration, but Sips' has the smallest mean squared error in adsorption and Freundlich's in desorption as shown in Table 4.1. When using the second method the four models behave similarly in both adsorption and desorption for this concentration ranges, nevertheless the model with the smallest mean squared error in both isotherms was Sips'. Similar behaviour of the models is attributed to the low concentration of tomato oleoresin in the fluid phase. From data analysed, nothing can be said about tomato oleoresin behaviour at higher concentrations as shown in Fig. 4.15.

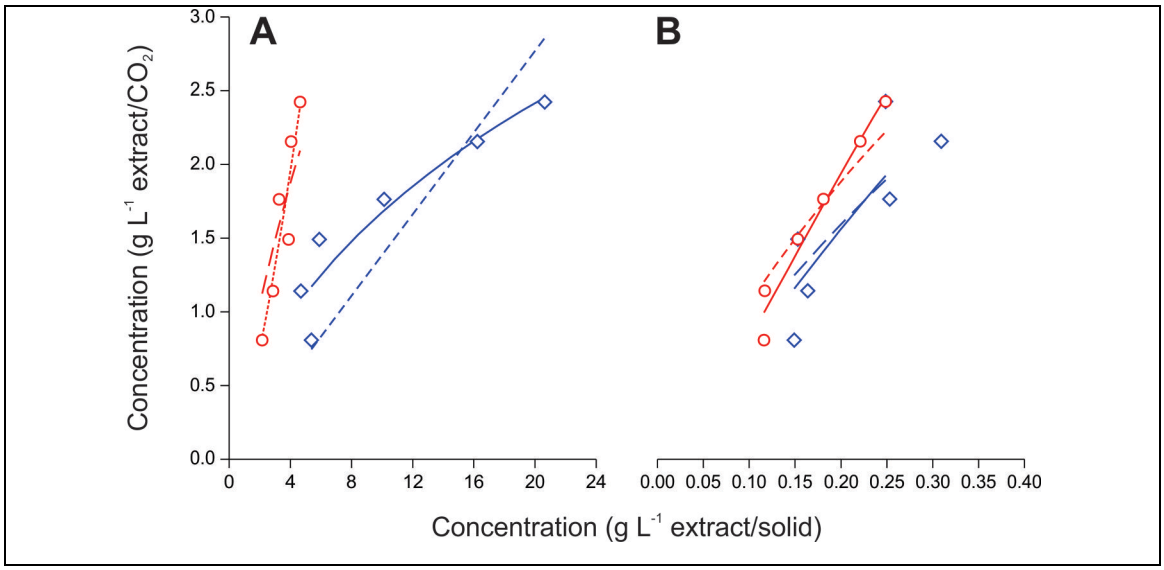

Figure 4.14: Best and worst fitted isotherm: **A** Concentration calculated with mass balance method, and **B** Concentration calculated with breakthrough curves method. Sips (——), Langmuir (— —), Freundlich (·····) and Lineal (– – – –). Adsorption (◇) and desorption (○).

Table 4.1: Isotherm models experimental parameters fitted by least square method, and their mean squared error (mse). With c_{fsat} = 8.52 g/L CO_2

	Adsorption			Desorption		
Model	K	n	mse	K	n	mse
Method 1						
Linear	0.1385	–	0.1714	0.4776	–	0.0615
Freundlich	0.4667	0.5498	0.0357	0.2843	1.3898	0.0445
Langmuir	0.0228	–	0.0815	0.0703	–	0.0842
Sips	0.0496	0.6929	0.0346	0.0279	1.7115	0.0448
Method 2						
Linear	7.6849	–	0.0960	9.5427	–	0.0163
Freundlich	7.2438	1.0431	0.0958	12.5491	0.8565	0.0117
Langmuir	1.1496	–	0.0996	1.4189	–	0.0366
Sips	1.572	1.2103	0.0929	3.1433	1.4711	0.0104

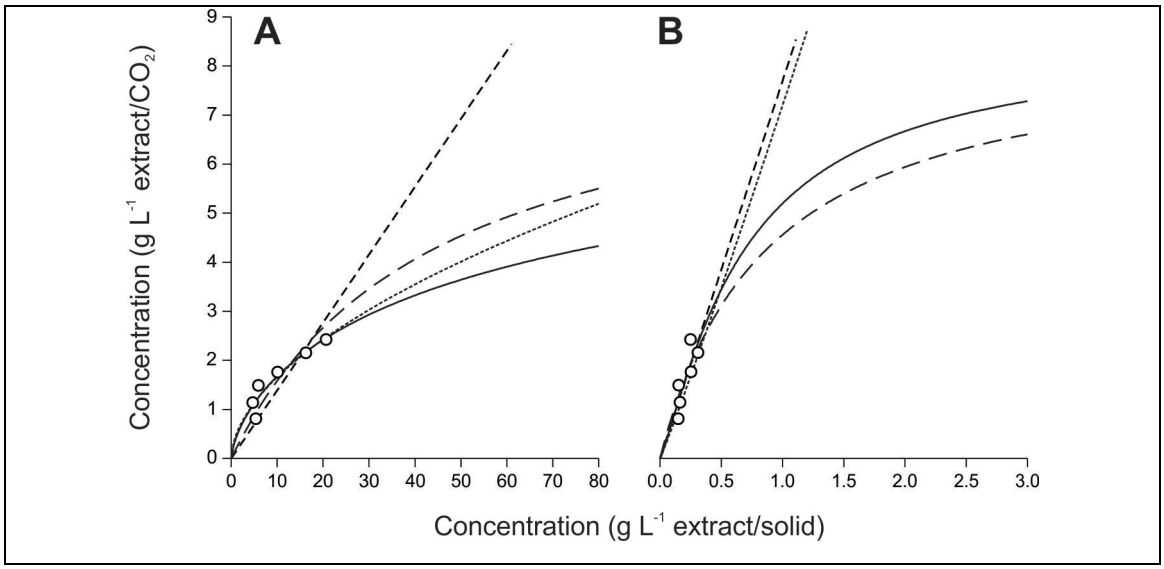

Figure 4.15: Prolongation of the four isotherm models: **A** data calculated with mass balance method in adsorption curves, and **B** data calculated with breakthrough curves method in adsorption curves. Sips (——), Langmuir (— —), Freundlich (---------) and Lineal (– – – –). Experimental data (○).

One factor that was not considered is the possibility of the oleoresin to change its saturation equilibrium due to concentration changes. This might happen because extraction conditions are different from working conditions, thus more soluble compounds could diminish their concentration in the static system while it is working. It is recommended to study both, the effect of time on the oleoresin quality, and the effect of changing the static system concentration.

5. CONCLUSIONS

This thesis contains both a review on sorption phenomena in separation processes using supercritical fluids, and experimental work on the partition of tomato oleoresin between SC CO_2 and selected chemical adsorbents. Firstly, it reviews the supercritical adsorption concept as it applies to gas adsorption, textile dyeing, soil remediation, adsorbent regeneration, and separation processes for mixtures. It is recommended to study the behaviour of natural mixtures with ideal adsorbents like silica gel, and also ideal solutes (pure solutes) with natural adsorbents.

The experimental part of the thesis compares adsorbents using hexane as the mobile phase, with the purpose of choosing the most appropriate for studying the equilibrium partition of tomato oleoresin between SC CO_2 and the selected adsorbent. In order to do this, activated carbon, microcrystalline cellulose, celite, silica gel, and chitosan in microspheres were assessed. Activated carbon was discarded because of its high affinity with tomato oleoresin, and microcrystalline cellulose and celite were discarded because of their lack of interaction with it. The selected adsorbents were silica gel that exhibited high affinity with tomato oleoresin, and chitosan in microspheres that exhibited low, yet noticeable, affinity.

While measuring equilibrium partition of tomato oleoresin between SC CO_2 and silica gels was not possible, the low interaction with the solute with chitosan in microspheres proved to be adequate for the purpose of this thesis. Volume of equilibration cell and packed column characteristics, made it impossible to measure silica gels equilibrium partition, thus silica gel was discarded. Reproducibility was tested and an irreversible oleoresin adsorption in chitosan was observed. Measurements using chitosan in microspheres were carried out using two methods, one based in mass balances, and other based in breakthrough curves. These two methods estimated different oleoresin concentrations in the solid phase. Furthermore, in both cases there were differences in the adsorption as compared to the desorption branch of the sorption isotherm. These differences were possibly due to difficulties in maintaining SC CO_2 saturated in the equilibration subsystem, and to fractionation of the oleoresin by the

adsorbent during the process. Microspheres were large and possibly contributed to axial dispersion in the packed bed which made estimations based on breakthrough curves imprecise. For the range of oleoresin concentration studied, the four isotherm models fitted well when using breakthrough analysis, while Freundilch's and Sips' fitted better when integrating differences the adsorbent and glass bead columns. Although this work suggests that chitosan in microspheres may not be an appropriate adsorbent for SC separation purposes, part of this conclusion is due to limitations of the methods used in it. Thus, it is recommended to study both, the effect of time on tomato oleoresin composition and quality. If fractionation is observed (i.e., if the carotenoid content in the oleoresin changes with time), it is suggested to apply the method based on mass balances.

REFERENCES

Ahmad, A. L., Chan, C. Y., Abd Shukor, S. R., & Mashitah, M. D. (2009). Adsorption kinetics and thermodynamics of β-carotene on silica-based adsorbent. *Chemical Engineering Journal*, *148*, 378–384.

Ambrogi, A., Cardarelli, D. A., & Eggers, R. (2002). Fractional extraction of paprika using supercritical carbon dioxide and on-line determination of carotenoids. *Journal of Food Science*, *67*, 3236–3241.

Ambrogi, A., Cardarelli, D. A., & Eggers, R. (2003). Separation of natural colorants using a combined high pressure extraction-adsorption process. *Latin American Applied Research*, *33*, 323–326.

Aranovich, G. L., & Donohue, M. D. (1996). Adsorption of supercritical fluids. *Journal of Colloid* and *Interface Science*, *180*, 537–541.

Bach, E., Cleve, E., & Schollmeyer, E. (2002). Past, present and future of supercritical fluid dieying technology - an overview. *Review of Progress in Coloration and Related Topics*, *32*, 88–102.

Bachu, S. (2000). Sequestration of CO_2 in geological media: criteria and approach for site selection in response to climate change. *Energy Conversion and Management*, *41*, 953–970.

Banchero, M. (2012). Supercritical fluid dyeing of synthetic and natural textiles - a review. Coloration *Technology*, *129*, 2–17.

Beltrame, P. L., Castelli, A., Selli, E., Mossa, A., Testa, G., Bonfatti, A. M., & Seves, A. (1997). Dyeing of cotton in supercritical carbon dioxide. *Dyes and Pigments*, *39*, 335–340.

Benyahia, F., & O'Neill, K. E. (2005). Enhanced voidage correlations for packed beds of various particle shapes and sizes. *Particulate Science and Technology*, *23*, 169–177.

Berglöf, T., Koskinen, W. C., & Kylin, H. (1998). Supercritical fluid extraction of metsulfuron methyl, sulfometuron methyl, and nicosulfuron from soils. *International Journal of Environmental Analytical Chemistry*, *70*, 37–45.

Bernal, J. L., Jiménez, J. J., Atienza, J., & Herguedas, A. (1996). Extraction of triallate from soil with supercritical carbon dioxide and determination by gas chromatography—atomic emission detection: Comparison with a solvent extraction procedure. *Journal of Chromatography A*, *754*, 257–263.

Brady, B. O., Kao, C.-P. C., Dooley, K. M., Knopf, F. C., & Gambrel, R. P. (1987). Supercritical extraction of toxic organics from soils. *Industrial & Engineering Chemistry Research*, *26*, 261–268.

Braida, I., Mattea, M., & Cardarelli, D. (2008). Extraction–adsorption–desorption process under supercritical condition as a method to concentrate antioxidants from natural sources. *The Journal of Supercritical Fluids*, *45*, 195–199.

Bramley, P. M. (2000). Is lycopene beneficial to human health? *Phytochemistry*, *54*, 233–236.

Brixie, J. M., & Boyd, S. A. (1994). Treatment of contaminated soils with organoclays to reduce leachable pentachlorophenol. *Journal of Environmental Quality*, *23*, 1283–1290.

Brunner, G., & Johannsen, M. (2006). New aspects on adsorption from supercritical fluid phases. *The Journal of Supercritical Fluids*, *38*, 181–200.

Cavalcante, A. M., Torres, L. G., & Coelho, G. L. V. (2005). Adsorption of ethyl acetate onto modified clays and its regeneration with supercritical CO_2. *Brazilian Journal of Chemical Engineering*, *22*, 75–82.

Chambers, A., Park, C., Baker, R. T. K., & Rodriguez, N. M. (1998). Hydrogen storage in *graphite* nanofibers. *The Journal of Physical Chemistry B*, *102*, 4253–4256.

Chen, P., Wu, X., Lin, J., & Tan, K. L. (1999). High H_2 uptake by alkali-doped carbon *nanotubes* under ambient pressure and moderate temperatures. *Science*, *285*, 91–93.

Choong, T. S. Y., Chuah, T. G., Yunus, R., & Yap, Y. H. T. (2010). Adsorption of β-carotene onto mesoporous carbon coated monolith in isopropyl alcohol and n-hexane *solution*: equilibrium and thermodynamic study. *Chemical Engineering Journal*, *164*, 178–182.

Chouchi, D., Barth, D., Reverchon, E., & Della Porta, G. (1996). Bigarade peel oil fractionation by supercritical carbon dioxide desorption. *Journal of Agricultural and Food Chemistry*, *44*, 1100–1104.

Chu, B. S., Baharin, B. S., Che Man, Y. B., & Quek, S. Y. (2004a). Separation of vitamin E from palm fatty acid distillate using silica: I Equilibrium of batch adsorption. *Journal of Food Engineering*, *62*, 97–103.

Chu, B. S., Baharin, B. S., Che Man, Y. B., & Quek, S. Y. (2004b). Separation of vitamin E from palm fatty acid distillate using silica: II Kinetics of batch adsorption. *Journal of* Food *Engineering*, *62*, 105–111.

Chu, B. S., Baharin, B. S., Che Man, Y. B., & Quek, S. Y. (2004c). Separation of vitamin E from palm fatty acid distillate using silica. III. Batch desorption study. *Journal of Food Engineering*, *64*, 1–7.

Clarkson, C. R., & Bustin, R. M. (2000). Binary gas adsorption/desorption isotherms: effect of moisture and coal composition upon carbon dioxide selectivity over methane. *International Journal of Coal Geology*, *42*, 241–271.

Coelho, G. L. V, Augusto, F., & Pawliszyn, J. (2001). Desorption of ethyl acetate from Adsorbent surfaces (organoclays) by supercritical carbon dioxide. *Industrial & Engineering Chemistry Research*, *40*, 364–368.

de Silva, P. N. K., Ranjith, P. G., & Choi, S. K. (2012). A study of methodologies for CO_2 storage capacity estimation of coal. *Fuel*, *91*, 1–15.

Dean, J. R., Barnabas, I. J., & Fowlis, I. A. (1995). Extraction of polycyclic aromatic hydrocarbons from highly contaminated soils : a comparison between soxhlet , microwave and supercritical fluid extraction techniques. *Analytical Proceedings Including Analytical Communications*, *32*, 305–308.

del Valle, J. M., & Aguilera, J. M. (1999). Revision: Extraccion con CO_2 a alta presion. Fundamentos y aplicaciones en la industria de alimentos. *Food Science and* Technology *International*, *5*, 1–24.

del Valle, J. M., & de la Fuente, J. C. (2006). Supercritical CO_2 extraction of oilseeds: review of kinetic and equilibrium models. *Critical Reviews in Food Science and Nutrition*, *46*, 131–160.

del Valle, J. M., & Urrego, F. A. (2012). Free solute content and solute-matrix interactions affect apparent solubility and apparent solute content in supercritical CO_2 extractions. A hypothesis paper. *The Journal of Supercritical Fluids*, *66*, 157–175.

Dettmer, K., & Engewald, W. (2002). Adsorbent materials commonly used in air analysis for adsorptive enrichment and thermal desorption of volatile organic compounds. *Analytical and Bioanalytical Chemistry*, *373*, 490–500.

Díez-Municio, M., Montilla, A., Herrero, M., Olano, A., & Ibáñez, E. (2011). Supercritical CO_2 impregnation of lactulose on chitosan: A comparison between scaffolds and microspheres form. *The Journal of Supercritical Fluids*, *57*, 73–79.

Dillon, A. C., Jones, K. M., Bekkedahl, T. A., Klang, C. H., Bethune, D. S., & Heben, M. J. (1997). Storage of hydrogen in single-walled carbon nanotubes. *Nature*, *386*, 377–379.

Dixon, A. G. (1988). Correlations for wall and particle shape effects on fixed bed bulk voidage. *The Canadian Journal of Chemical Engineering*, *66*, 705–708.

Dupeyron, S., Dudermel, P.-M., Couturier, D., Guarini, P., & Delattre, J.-M. (1999). Extraction of polycyclic aromatic hydrocarbons from soils: A comparison between focused microwave assisted extraction, supercritical fluid extraction, subcritical solvent extraction, sonication and soxhlet techniques. *International Journal of Environmental Analytical Chemistry*, *73*, 191–210.

Erkey, C., Madras, G., Orejuela, M., & Akgerman, A. (1993). Supercritical carbon dioxide extraction of organics from soil. *Environmental Science & Technology*, *27*, 1225–1231.

Frost, R. L., Zhou, Q., He, H., & Xi, Y. (2008). An infrared study of adsorption of para-nitrophenol on mono-, di- and tri-alkyl surfactant intercalated organoclays. *Spectrochimica Acta. Part A, Molecular and Biomolecular Spectroscopy*, *69*, 239–44.

Germain, J. C., del Valle, J. M., & de la Fuente, J. C. (2005). Natural convection retards supercritical CO_2 extraction of essential oils and lipids from vegetable substrates. *Industrial & Engineering Chemistry Research*, *44*, 2879–2886.

Gómez-Prieto, M. S., Caja, M. M., Herraiz, M., & Santa-María, G. (2003). Supercritical fluid extraction of all-trans-lycopene from tomato. *Journal of Agricultural and Food Chemistry*, *51*, 3–7.

Gregorowicz, J. (2005). Adsorption of eicosane and 1,2-hexanediol from supercritical carbon dioxide on activated carbon and chromosorb. *Fluid Phase Equilibria*, *238*, 142–148.

Guiochon, G., & Tarafder, A. (2011). Fundamental challenges and opportunities for preparative supercritical fluid chromatography. *Journal of Chromatography A*, *1218*, 1037–1114.

Guzel, B., & Akgerman, A. (2000). Mordant dyeing of wool by supercritical processing. *The Journal of Supercritical Fluids*, *18*, 247–252.

Hall, F. E., Zhou, C., Gasem, K. A. M., Robinson Jr, R. L., & Yee, D. (1994). Adsorption of pure methane, nitrogen, and carbon dioxide and their binary mixtures on wet fruitland coal. In *Eastern Regional Conference & Exhibition of the Society of Petroleum Engineers* (pp. 329–344). Charleston, WV.

Hawthorne, S. B., & Miller, D. J. (2003). Evidence for very tight sequestration of BTEX compounds in manufactured gas plant soils based on selective supercritical fluid extraction and soil/water partitioning. *Environmental Science & Technology*, *37*, 3587–3594.

Heaton, D. M., Bartle, K. D., Myers, P., & Clifford, A. A. (1996). Use of modifier as trapping fluid in preparative supercritical fluid chromatography. *Journal of Chromatography A*, *753*, 306–311.

Henry, L. K., Catignani, G. L., & Schwartz, S. J. (1998). Oxidative degradation kinetics of lycopene , lutein , and 9-cis and all-trans β-carotene. *Journal of the American Oil* Chemists' *Society*, *75*, 823–829.

Hou, A., Chen, B., Dai, J., & Zhang, K. (2010). Using supercritical carbon dioxide as solvent to replace water in polyethylene terephthalate (PET) fabric dyeing procedures. *Journal of Cleaner Production*, *18*, 1009–1014.

Huang, J., Wang, X., Jin, Q., Liu, Y., & Wang, Y. (2007). Removal of phenol from aqueous solution by adsorption onto OTMAC-modified attapulgite. *Journal of* Environmental *Management*, *84*, 229–36.

IPCC. (2005). IPCC Special report on carbon dioxide capture and storage: Carbon dioxide capture and storage. (B. Metz, O. Davidson, H. de Conick, M. Loos, & L. Meyer, Eds.). Cambridge, UK and New York, NY, USA: Cambridge University Press.

Jüntgen, H. (1977). New applications for carbonaceous adsorbents. *Carbon*, *15*, 273–283.

Kikic, I., Alessi, P., Cortesi, A., Macnaughton, S. J., Foster, N. R., & Spicka, B. (1996). An experimental study of supercritical adsorption equilibria of salicylic acid on *activated* carbon. *Fluid Phase Equilibria*, *117*, 304–311.

Krooss, B. M., van Bergen, F., Gensterblum, Y., Siemons, N., Pagnier, H. J. M., & David, P. (2002). High-pressure methane and carbon dioxide adsorption on dry and moisture-equilibrated Pennsylvanian coals. *International Journal of Coal Geology*, *51*, 69–92.

Lee, L. L., & Cochran, H. D. (1992). Adsorption from supercritical fluids. In E. Kiran & J. F. Brennecke (Eds.), *Supercritical Fluids Engineering Science* (pp. 188–200). Washington, DC: American Chemical Society.

Liu, F., Ellett, K., Xiao, Y., & Rupp, J. A. (2013). Assessing the feasibility of CO_2 storage in the New Albany Shale (Devonian–Mississippian) with potential enhanced gas recovery using reservoir simulation. *International Journal of Greenhouse Gas Control*, *17*, 111–126.

Liu, Z.-T., Zhang, L., Liu, Z., Gao, Z., Dong, W., Xiong, H., Peng, Y. & Tang, S. (2006). Supercritical CO_2 dyeing of ramie fiber with disperse dye. *Industrial & Engineering* Chemistry *Research*, *45*, 8932–8938.

Lo, I., & Yang, X. (2001). Use of organoclay as secondary containment for gasoline storage tanks. *Journal of Environmental Engineering*, *127*, 154–161.

Lucas, S., Cocero, M. J., Zetzl, C., & Brunner, G. (2004). Adsorption isotherms for ethylacetate and furfural on activated carbon from supercritical carbon dioxide. *Fluid Phase Equilibria*, *219*, 171–179.

Macnaughton, S. J., & Foster, N. R. (1995). Supercritical adsorption and desorption behavior of DDT on activated carbon using carbon dioxide. *Industrial & Engineering Chemistry Research*, *34*, 275–282.

Madras, G., Erkey, C., & Akgerman, A. (1993). Supercritical fluid regeneration of activated carbon loaded with heavy molecular weight organics. *Industrial & Engineering Chemistry Research*, *32*, 1163–1168.

Madras, G., Erkey, C., & Akgerman, A. (1994). Supercritical extraction of organic contaminants from soil combined with adsorption onto activated carbon. *Environmental Progress*, *13*, 45–50.

McCabe, W., & Smith, J. (1969). Lixiviación y Extracción. In *Operaciones básicas de* Ingeniería *Química* (pp. 735–780). Barcelona, Spain: Editorial Reverté S.A.

Miller, L. (2012). Preparative enantioseparations using supercritical fluid chromatography. *Journal of* Chromatography *A*, *1250*, 250–255.

Miller, L. (2014). Use of dichloromethane for preparative supercritical fluid chromatographic enantioseparations. *Journal of Chromatography A, 1363*, 323-330.

Miller, L., & Potter, M. (2008). Preparative chromatographic resolution of racemates using HPLC and SFC in a pharmaceutical discovery environment. *Journal of*

Chromatography. *B, Analytical Technologies in the Biomedical and Life Sciences*, *875*, 230–236.

Monteiro de Castro, M., Martínez-Escandell, M., Molina-Sabio, M., & Rodríguez-Reinoso, F. (2010). Hydrogen adsorption on KOH activated carbons from mesophase pitch containing Si, B, Ti or Fe. *Carbon*, *48*, 636–644.

Murata, K., Kaneko, K., Kanoh, H., Kasuya, D., Takahashi, K., Kokai, F., Yudasaka, M. & Iijima, S. (2002). Adsorption mechanism of supercritical hydrogen in internal and interstitial nanospaces of single-wall carbon nanohorn assembly. *The Journal of Physical Chemistry B*, *106*, 11132–11138.

Nagpal, V., & Guigard, S. E. (2005). Remediation of flare pit soils using supercritical fluid extraction. *Journal of Environmental Engineering and Science*, *4*, 307–318.

NIST. (2011). Carbon dioxide. Retrieved September 02, 2013, from http://webbook.nist.gov/cgi/cbook.cgi?ID=C124389&Mask=4#Thermo-Phase

Ollanketo, M., Hartonen, K., Riekkola, M.-L., Holm, Y., & Hiltunen, R. (2001). Supercritical carbon dioxide extraction of lycopene in tomato skins. *European Food Research and Technology*, *212*, 561–565.

Özcan, A. S., Clifford, A. A., Bartle, K. D., Broadbent, P. J., & Lewis, D. M. (1998a). Dyeing of modified cotton fibres with disperse dyes from supercritical carbon dioxide. *Journal of the Society of Dyers and Colourists*, *114*, 169–173.

Özcan, A. S., Clifford, A. A., Bartle, K. D., & Lewis, D. M. (1998b). Dyeing of cotton fibres with disperse dyes in supercritical carbon dioxide. *Dyes and Pigments*, *36*, 103–110.

Özcan, A. S., & Özcan, A. (2005). Adsorption behavior of a disperse dye on polyester in supercritical carbon dioxide. *The Journal of Supercritical Fluids*, *35*, 133–139.

Pantoula, M., von Schnitzler, J., Eggers, R., & Panayiotou, C. (2007). Sorption and swelling in glassy polymer/carbon dioxide systems. Part II-Swelling. *The Journal of Supercritical Fluids*, *39*, 426–434.

Park, S.-C., Tuma, D., Kim, S., Lee, Y., & Shim, J.-J. (2010). Sorption of C. I. disperse red 60 in polystyrene and PMMA films and polyester and nylon 6 textiles in the presence of supercritical carbon dioxide. *Korean Journal of Chemical Engineering*, *27*, 299–309.

Park, S.-J., & Yeo, S.-D. (1999). Supercritical extraction of phenols from organically modified smectite. *Separation Science and Technology*, *34*, 101–113.

Pashin, J. C., & McIntyre, M. R. (2003). Temperature–pressure conditions in coalbed methane reservoirs of the Black Warrior basin: implications for carbon sequestration and enhanced coalbed methane recovery. *International Journal of Coal Geology*, *54*, 167–183.

Perera, M. S. a., Ranjith, P. G., Choi, S. K., Bouazza, A., Kodikara, J., & Airey, D. (2010). A review of coal properties pertinent to carbon dioxide sequestration in coal seams: with special reference to Victorian brown coals. *Environmental Earth Sciences*, *64*, 223–235.

Periago, M. J., Rincón, F., Agüera, M. D., & Ros, G. (2004). Mixture approach for optimizing lycopene extraction from tomato and tomato products. *Journal of Agricultural and Food Chemistry*, *52*, 5796–5802.

Puri, R., & Yee, D. (1990). Enhanced coalbed methane recovery. In *SPE Anual Technical Conference and Exhibition* (pp. 193–203). New Orleans, LA.

Ramírez, P., García-Risco, M. R., Santoyo, S., Señoráns, F. J., Ibáñez, E., & Reglero, G. (2006). Isolation of functional ingredients from rosemary by preparative-supercritical fluid chromatography (Prep-SFC). *Journal of Pharmaceutical and Biomedical Analysis*, *41*, 1606–1613.

Ramírez, P., Santoyo, S., García-Risco, M. R., Señoráns, F. J., Ibáñez, E., & Reglero, G. (2007). Use of specially designed columns for antioxidants and antimicrobials enrichment by preparative supercritical fluid chromatography. *Journal of Chromatography*, *1143*, 234–42.

Rao, A. V, & Rao, L. G. (2007). Carotenoids and human health. *Pharmacological* Research, *55*, 207–216.

Reichle, D., Houghton, J., Kane, B., Ekmann, J. Carbon sequestration research and development. 1999. Office of Fosil Energy, DOE.

Reverchon, E., & Iacuzio, G. (1997). Supercritical desorption of bergamot peel oil from silica gel—Experiments and mathematical modelling. *Chemical Engineering Science*, *52*, 3553–3559.

Sahle-Demessie, E., & Richardson, T. (2000). Cleaning up pesticide contaminated soils: comparig effectiveness of supercritical fluid extraction with solvent extraction and low temperature thermal desorption. *Environmental Technology*, *21*, 447–456.

Saldaña, M., Temelli, F., Guigard, S., Tomberli, B., & Gray, C. (2010). Apparent solubility of lycopene and β-carotene in supercritical CO_2, CO_2 +ethanol and CO_2 +canola oil using dynamic extraction of tomatoes. *Journal of Food Engineering*, *99*, 1–8.

Salgın, U., Yıldız, N., & Çalımlı, A. (2004). Desorption of salicylic acid from modified bentonite by using supercritical fluids in packed bed column. *Separation Science and Technology*, *39*, 2677–2694.

Salimi, A., Fatemi, S., Zakizadeh Nei Nei, H., & Safaralie, A. (2008). Mathematical modeling of supercritical extraction of valerenic acid from *Valeriana officinalis L*. *Chemical Engineering & Technology*, *31*, 1470–1480.

Schleussinger, A., Ohlmeier, B., Reiss, I., & Schulz, S. (1996). Moisture Effects on the Cleanup of PAH-Contaminated Soil with Dense Carbon Dioxide. *Environmental Science & Technology*, *30*, 3199–3204.

Schmidt, A., Bach, E., & Schollmeyer, E. (2003). Supercritical fluid dyeing of cotton modified with 2,4,6-trichloro-1,3,5-triazine. *Coloration Technology*, *119*, 31–36.

Seidel-Morgenstern, A. (2004). Experimental determination of single solute and competitive adsorption isotherms. *Journal of Chromatography A*, *1037*, 255–272.

Shen, Z., Mishra, V., Imison, B., Palmer, M., & Fairclough, R. (2002). Use of adsorbent and supercritical carbon dioxide to concentrate flavor compounds from orange oil. *Journal of Agricultural and Food Chemistry*, *50*, 154–160.

Shi, J., Khatri, M., Xue, S. J., Mittal, G., Ma, Y., & Li, D. (2009). Solubility of lycopene in *supercritical* CO_2 fluid as affected by temperature and pressure. *Separation and Purification Technology*, *66*, 322–328.

Shieh, Y.-T., & Liu, K.-H. (2003). The effect of carbonyl group on sorption of CO_2 in glassy *polymers*. *The Journal of Supercritical Fluids*, *25*, 261–268.

Shu, L., & *Su*, Y. (2002). Bencene vapor sorption by organobentonites from ambient air. *Clays and Clay Minerals*, *50*, 421–427.

Siriwardane, H. J., Gondle, R. K., & Smith, D. H. (2009). Shrinkage and swelling of coal induced by desorption and sorption of fluids: Theoretical model and interpretation of a *field* project. *International Journal of Coal Geology*, *77*, 188–202.

Škerget, M., & Knez, Z. (2007). Supercritical fluid adsorption and desorption of lipids on various adsorbents. *Acta Chimica Slovenica*, *54*, 688–692.

Stanton, R. W., Burruss, R. C., Flores, R. M., & Warwick, P. D. (2001). CO_2 Adsorption in low-rank coals: progress toward assessing the nation-wide capacity to store CO_2 in the subsurface. In *Proceedings of the Eighteenth Annual International Pittsburgh Coal Conference* (pp. 1–2). Newcastle, NSW, Australia.

Stevens, S. H., Kuuskraa, V. A., Gale, J., & Beecy, D. (2001). CO_2 injection and sequestration in depleted oil and gas fields and deep coal seams: Worldwide potential and costs. *Environmental Geosciences*, *8*, 200–209.

Ströbel, R., Garche, J., Moseley, P. T., Jörissen, L., & Wolf, G. (2006). Hydrogen storage by carbon materials. *Journal of Power Sources*, *159*, 781–801.

Su, B., Xing, H., Han, Y., Yang, Y., Ren, Q., & Wu, P. (2009). Adsorption equilibria of cis-5,8,11,14,17-eicosapentaenoic acid ethyl ester and cis-4,7,10,13,16,19-docosahexaenoic acid ethyl ester on C18-bonded silica from supercritical carbon dioxide. *Journal of Chemical & Engineering Data*, *54*, 2906–2913.

Subra, P., Vega-Bancel, A., & Reverchon, E. (1998). Breakthrough curves and adsorption isotherms of terpene mixtures in supercritical carbon dioxide. *The Journal of Supercritical Fluids*, *12*, 43–57.

Sudibandriyo, M. (2011). High pressure adsorption of methane and hydrogen at 25 ^{o}C on activated carbons prepared from coal and coconut shell. *International Journal of Engineering & Technology*, *11*, 79–85.

Sunarso, J., & Ismadji, S. (2009). Decontamination of hazardous substances from solid matrices and liquids using supercritical fluids extraction: a review. *Journal of Hazardous Materials*, *161*, 1–20.

Tan, C. S., & Liou, D. C. (1988). Desorption of ethyl acetate from activated carbon by supercritical carbon dioxide. *Industrial & Engineering Chemistry Research*, *27*, 988–991.

Tan, C. S., & Liou, D. C. (1989a). Regeneration of activated carbon loaded with toluene by supercritical carbon dioxide. *Separation Science and Technology*, *24*, 111–127.

Tan, C. S., & Liou, D. C. (1989b). Supercritical regeneration of activated carbon loaded with benzene and toluene. *Industrial & Engineering Chemistry Research*, *28*, 1222–1226.

Tian, S., Zhu, L., & Shi, Y. (2004). Characterization of sorption mechanisms of VOCs with organobentonites using a LSER approach. *Environmental Science & Technology*, *38*, 489–95.

Tomasko, D. L., Li, H., Liu, D., Han, X., Wingert, M. J., Lee, L. J., & Koelling, K. W. (2003). A review of CO_2 applications in the processing of polymers. *Industrial & Engineering Chemistry Research*, *42*, 6431–6456.

Urrego, F. A., del Valle, J. M., & de la Fuente, J. C. (2011). Carotenoid partition between supercritical CO_2 and red peppers. In *International Congress of Engineering and Food 11*. Athen, Greece.

Urrego, F. A., del Valle, J. M., & de la Fuente, J. C. (2012). Carotenoid partition between vegetable-oil-modified or pure supercritical carbon dioxide and red peppers. In *International Symposium of Supercritical Fluids 2012*. San Francisco, CA.

van der Kraan, M., Fernandez Cid, M. V, Woerlee, G. F., Veugelers, W. J. T., & Witkamp, G. J. (2007). Dyeing of natural and synthetic textiles in supercritical carbon dioxide with disperse reactive dyes. *The Journal of Supercritical Fluids*, *40*, 470–476.

Vasanth Kumar, K., Monteiro de Castro, M., Martinez-Escandell, M., Molina-Sabio, M., & Rodriguez-Reinoso, F. (2010). A continuous binding site affinity distribution function from the Freundlich isotherm for the supercritical adsorption of hydrogen on activated carbon. *The Journal of Physical Chemistry C*, *114*, 13759–13765.

Viete, D. R., & Ranjith, P. G. (2006). The effect of CO_2 on the geomechanical and permeability behaviour of brown coal: Implications for coal seam CO_2 sequestration. *International Journal of Coal Geology*, *66*, 204–216.

Volzone, C., Rinaldi, J. O., & Ortiga, J. (2006). Retention of gases by hexadecyltrimethylammonium-montmorillonite clays. *Journal of Environmental Management*, *79*, 247–52.

von Schnitzler, J., & Eggers, R. (1999). Mass transfer in polymers in a supercritical CO_2 -atmosphere. *The Journal of Supercritical Fluids*, *16*, 81–92.

West, B. L., Kazarian, S. G., Vincent, M. F., Brantley, N. H., & Eckert, C. A. (1998). Supercritical fluid dyeing of PMMA films with azo-dyes. *Journal of Applied Polymer Science*, 69, 911–919.

White, C. M., Smith, D. H., Jones, K. L., Goodman, A. L., Jikich, S. A., LaCount, R. B., DuBose, S.B., Ozdemir, E., Morsi, B. I., & Schroeder, K. T. (2005). Sequestration of carbon dioxide in coal with enhanced coalbed methane recovery – A review. *Energy and Fuels*, *19*, 659 – 724.

White, C. M., Strazisar, B. R., Granite, E. J., Hoffman, J. S., & Pennline, H. W. (2003). Separation and capture of CO_2 from large stationary sources and sequestration in

geological formations—coalbeds and deep saline aquifers. *Journal of the Air & Waste Management Association*, *53*, 645–715.

Wright, B. W., Wright, C. W., & Fruchter, J. S. (1989). Supercritical fluid extraction of coal tar contaminated soil samples. *Energy and Fuels*, *3*, 474–480.

Wu, C., Gao, Q., Hu, J., Chen, Z., & Shi, W. (2009). Rapid preparation, characterization and hydrogen storage properties of pure and metal ions doped mesoporous MCM-41. *Microporous and Mesoporous Materials*, *117*, 165–169.

Xing, H., Su, B., Ren, Q., & Yang, Y. (2009). Adsorption equilibria of artemisinin from supercritical carbon dioxide on silica gel. *The Journal of Supercritical Fluids*, *49*, 189–195.

Young, T. M., & Weber, W. J. (1997). Equilibrium and rate study of analyte-matrix interactions in supercritical fluid extraction. *Analytical Chemistry*, *69*, 1612–1619.

Zheng, Q. R., Gu, A. Z., Lu, X. S., & Lin, W. S. (2005). Adsorption equilibrium of supercritical hydrogen on multi-walled carbon nanotubes. *The Journal of* Supercritical *Fluids*, *34*, 71–79.

Zhou, F., Hou, W., Allinson, G., Wu, J., Wang, J., & Cinar, Y. (2013). A feasibility study of ECBM recovery and CO_2 storage for a producing CBM field in Southeast Qinshui Basin, China. *International Journal of Greenhouse Gas Control*, *19*, 26–40.

Zhou, M., Trubey, R. K., Keil, Z. O., & Sparks, D. L. (1997). Study of the Effects of Environmental Variables and Supercritical Fluid Extraction Parameters on the Extractability of Pesticide Residues from Soils Using a Multivariate Optimization Scheme. *Environmental Science & Technology*, *31*, 1934–1939.

Zhou, Q., Frost, R. L., He, H., Xi, Y., & Liu, H. (2007). Adsorbed para-nitrophenol on HDTMAB organoclay-a TEM and infrared spectroscopic study. *Journal of Colloid and Interface Science*, *307*, 357–63.

Zhou, Q., Frost, R. L., He, H., Xi, Y., & Zbik, M. (2007). TEM, XRD, and thermal stability of adsorbed paranitrophenol on DDOAB organoclay. *Journal of Colloid and Interface Science*, *311*, 24–37.

Zhou, Y., & Zhou, L. (1996). Experimental study on high-pressure adsorption of hydrogen on activated carbon. *Science in China (Series B)*, *39*, 598–607.

Zhu, R., Zhu, J., Ge, F., & Yuan, P. (2009). Regeneration of spent organoclays after the sorption of organic pollutants: A review. *Journal of Environmental Management*, *90*(11), 3212–3216.

Zubizarreta, L., Gomez, E. I., Arenillas, A., Ania, C. O., Parra, J. B., & Pis, J. J. (2008). H_2 storage in carbon materials. *Adsorption*, *14*, 557–566.

Zuknik, M. H., Norulaini, N., & Omar, M. (2012). Supercritical carbon dioxide extraction of lycopene: A review. *Journal of Food Engineering*, *112*, 253–262.

NOMENCLATURE

c_f^i	Inicial concentration in the fluid phase (g/L)
c_f	Concentration in the fluid phase (g/L)
$c_{l,0}$	Liquid concentration at t = 0 (mg/L)
$c_{l,t}$	Liquid concentration at time t (mg/L)
c_s^i	Initial concentration in solid (g/L)
c_s	Concentration in solid (g/L)
$c_{s,t}$	Concentration in solid at time t for hexane experiments (mg/g)
c_{sat}	Saturation concentration in the fluid phase (g/L)
K	Partition coefficient for isotherm models (–)
L	Column length (mm)
n	Fitted parameter for isotherm models (–)
t_R	Retention time (min)
u	Superficial velocity (mm/s)
V	Volume (L)
W	Adsorbent weight (g)

Greek letters

ε	Porosity (–)

Subscritps

F	Freundlich
L	Langmuir
S	Sips

APPENDIXES

APPENDIX A: FRONTAL ANALYSIS IN STEPS

With the aim of obtaining data for the entire isotherm, frontal analysis can be done for increasing concentrations of solute in the fluid phase entering the column. Once the exit stream has reached the concentration of the inlet stream (equilibrium has been reached in the column), the input concentration is increased, and so it continues until the maximum concentration desired. The desorption procedure is similar, but decreasing progressively the input concentration, waiting until equilibrium at each concentration is reached. The response of the spectrophotometer should be like Figure A.1.

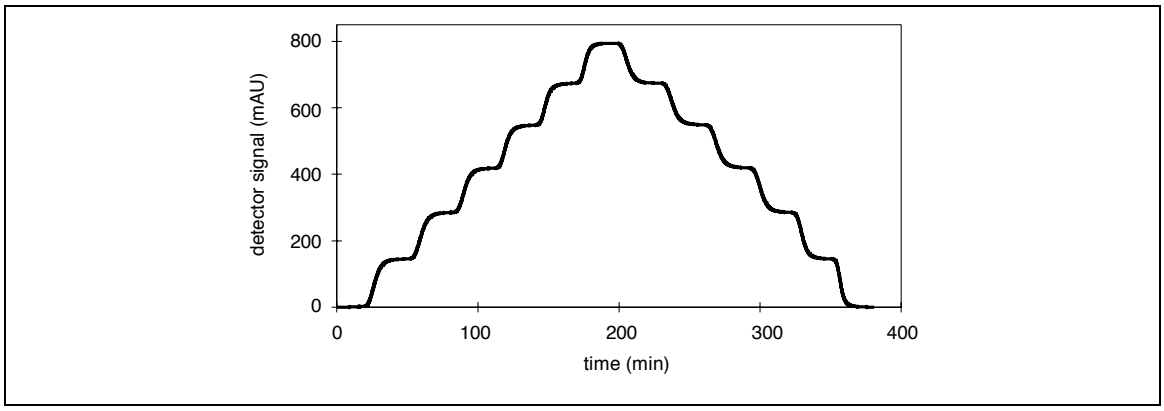

Figure A.1: Frontal analysis in steps.

APPENDIX B: POROSITY ESTIMATION

Packed bed porosity was estimated by using eqn. A.1 and A.2 obtained by Benyahia & O'Neill (2005), and Dixon (1988) respectively, and parameters detailed in Table A.1. The considered porosity was ε =0.425.

$$\varepsilon = 0.390 + \frac{1.740}{\left(\frac{d_t}{d_p}+1.140\right)^2} \quad \text{(A.1)}$$

$$\varepsilon = 0.400 + 0.050 \cdot \left(\frac{d_p}{d_t}\right) + 0.412 \cdot \left(\frac{d_p}{d_t}\right)^2 \quad \text{(A.2)}$$